DEVELOPMENT OF AN INDUCTIVE MAGNETOHYDRODYNAMIC GENERATOR

Roberto Pintus

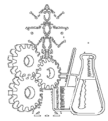

Università degli Studi di Cagliari
Dottorato di Ricerca in Ingegneria Industriale
XXIII Ciclo

DEVELOPMENT OF AN INDUCTIVE MAGNETOHYDRODYNAMIC GENERATOR

Roberto Pintus

Supervisor: Prof. Augusto Montisci

Università degli Studi di Cagliari
Dottorato di Ricerca in Ingegneria Industriale
XXIII Ciclo
ING-IND/31 ELETTROTECNICA

Dedicated to my parents

Acknowledgements

First and foremost, I would like to acknowledge Augusto Montisci, my supervisor, who pointed me toward this field of study and kept me on track. A special thanks to Massimo Camplani, Barbara Cannas, Sara Carcangiu, Alessandra Fanni, Anna Mereu, Fabio Pisano, Giuliana Sias, Mariangela Usai and to many of my colleagues for their support during these three years. Part of this dissertation has been completed at the Department of Mathematics University of Glasgow. I would like to acknowledge Dr Radostin D. Simitev, my supervisor in this foreign experience, for his support and his collaboration. Finally, I'd like to thank my family and friends for their continued support through this arduous work. It is only because of all these people that this document was completed.

Contents

List of Figures

List of Tables

Chapter 1

Introduction

In the last years the rapid rise in the use of electric power has raised the problem how to provide the power increases. From sector studies the total electrical power consumption has almost doubled in the last twenty years [9]. The problem of finding appropriate technologies to produce cheap energy and ensure the right standard of environmental compatibility, has in recent years led to an increase in technological progress. Nowadays electrical energy is the form of energy to which all other forms of energy may be converted. It is easy to transport, easy to control and easy to transform. Most of the times, however, energy can be converted into electricity only through many intermediate transformations, which leads to limitations in efficiency, reliability, and compactness. The critical point in general in the energy conversion is the combination of heat and mechanical energy of the conversion system, which limits the maximum temperature involved. To avoid the mechanical limitations it seems promising to convert directly heat into electricity. In this chapter I present a general description of the conventional conversion systems an their limitations.

1.1 Thermodynamic energy conversion

The electricity generation process, most often, is characterised by the transition of primary or secondary energy, from thermal to mechanical and then

to electricity. At the current state of development, most of the power plants are based on processes known as conventional. The production of electricity, through conventional forms or commercial of primary energy, concern only the hydroelectric and thermal power station, where the thermal power stations are different for use of primary source (usually fossil fuels such as natural gas, oil, coal, etc., wood and biomass, municipal or industrial solid wast, etc., or nuclear fuels and more rarely geothermal energy). In the hydroelectric power generation, mechanical energy, in different forms (kinetic, potential and pressure) from flowing fluid, is converted into electricity thanks to a water turbine and an alternator. In the thermal power plants the thermal energy is converted into mechanical energy and from this machine the mechanical energy into electricity. The majority of thermal power plants are powered by fuels, usually fossil or nuclear. In the figure 1.1 the necessary processes to product the electricity are shown. Apart some cases, such as power plants that use thermal energy available in nature (primarily solar and geothermal), the form of energy at the base of each of processes is the chemical potential energy of the fuel.

The potential energy of the fossil fuel is converted into heat energy through a chemical exothermic reaction (combustion), characterized by generation of thermal energy equivalent, in absolute value, to the enthalpy variation for the same reaction. In the case of nuclear fuels there is a fission reaction. The heat is then transmitted to elastic working fluid evolving in appropriate machines (usually gas turbine or reciprocating engine) producing mechanical work. In that case, it has converted thermal energy to mechanical (thermodynamics conversion). The mechanical work produced is finally transferred to an electric generator, which operates the last conversion of energy in electric form. It should be noted that in any conversion process one can not fully convert the energy from one form to another, each of the steps being characterized by a conversion efficiency, a coefficient that takes into account the fraction of the energy initially available, which is converted in the desired form.

1.1.1 Limits of thermodynamic energy conversion

In terms of performance, the overall process of thermal use is very expensive. In the conventional thermoelectric converters this is generally due to thermodynamic, technological and economic limitations. Here it will be called the most important aspects.

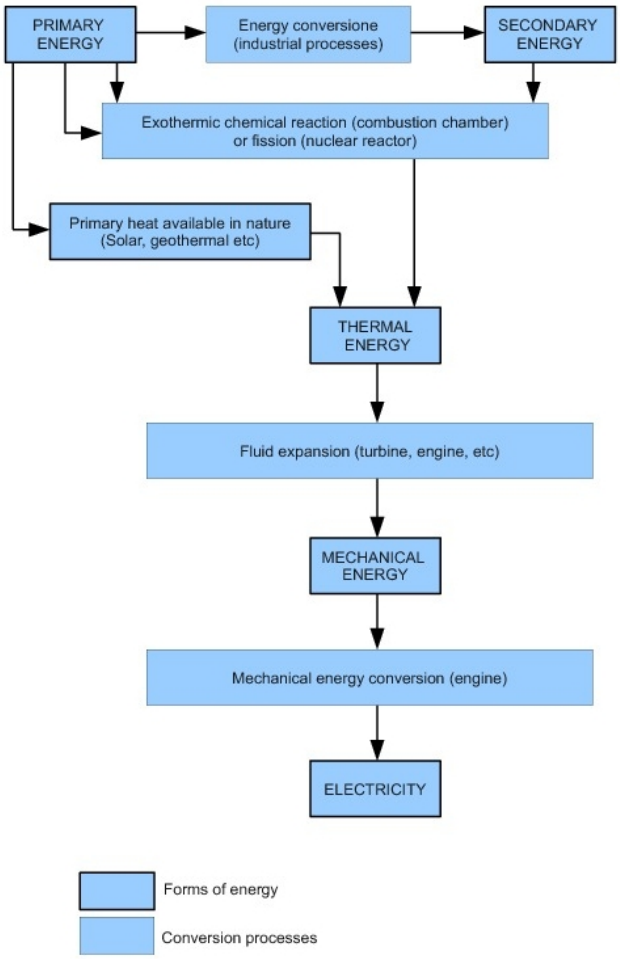

Figure 1.1: Stages of energy conversion and intermediate forms of energy conversion in conventional thermodynamics system

Thermodynamic limits

Today, most electrical energy is obtained from conventional fuels such as coal and gasoline or nuclear fuel such as uranium and thorium, through the service of heat engines. Although the heat engine is only one stage of many in

a conventional process, most of the losses occur there. Up to now, and probably for a long time to come, the generation of large-scale electrical power from thermal energy has required an intermediate step involving mechanical energy (see figure 1.1). The thermal energy from the primary source is used to raise steam. This steam is then fed onto a steam-turbine which is shaft-coupled to an electrical generator. In a typical central power plant, the efficiency of the boiler and the thermodynamic efficiency of the steam turbine are about 90% each, whereas the electrical efficiency of the generator is often around 98%, while the efficiency of the heat engine is usually below 45%. As the system works over a thermodynamic cycle the conversions efficiency of the process are restricted by the well-known Carnot limitations [28]. The Carnot efficiency is the maximum efficiency of an ideal heat engine which takes heat from a hot source at an absolute temperature T_h and releases it to a cold sink at a temperature T_c after doing work. This efficiency is given by

$$\eta_c = 1 - T_c / T_h; \tag{1.1}$$

The efficiency depends on two factors: the high temperature of a hot source and the cold temperature. The lowest temperature is limited by the temperature of the environment. Normally the lowest temperature available is in the range of 10-20°C. The maximum temperature is limited for obvious mechanical and metallurgical resistance reasons. As shown in figure 1.2, in the case of a cold source temperature of 300 K, the Carnot efficiency increases with the inlet temperature of the working fluid.

It must be emphasised that figure represents the maximum efficiency theoretically possible. Efficiency realised in practice is usually only about 60% of this theoretical maximum. In fact, in the steam power plant where the inlet temperatures are on the order of 550°C, in practice the conversion efficiency is only around 40%. Hence, the works to improve the overall efficiency of conventional power stations has been based on raising the inlet temperature. Obviously such developments are severely restricted by material limitations. Nowadays, gas turbines are the technologies that can work to the highest value of temperature cycle, with values around 1500 K [5]. These technologies are usually used as a topper in a combined cycle gas turbine (CCGT) plant [14]; a gas turbine generator produces electricity and the waste heat is used to make steam to generate additional electricity via a steam turbine. The Carnot efficiency for a thermal engine that works on those temperatures is about 80%.

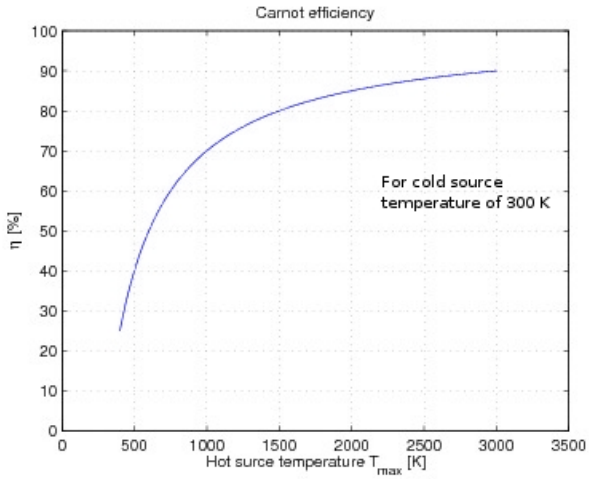

Figure 1.2: Carnot efficiency as a function of temperature

This means that, theoretically, can be transformed into work 80% of the input thermal energy. In practice most combined cycle units, especially the large units, have efficiencies of 55-60%.

Technology limits

From the equation 1.1 it is deduced that the efficiency of Carnot cycle depends only on temperatures. Regarding the limits on these temperatures, it should be noted that the T_{min} is linked to environmental conditions, or rather the minimum temperature cycle is considered equal to the external environment temperature. The T_{max} that affect the performance of the machine according to the law shown in the figure 1.2, has mainly a technological limit. This limit is related to the resistance of materials at high temperatures and high mechanical stress when it is working. In particular, for steam power plants, it should be noted, although in the furnace of the steam generator it is possible to reach temperatures of 2000°C, the turbine blades can not operate at more than 500-550°C. In gas turbines such temperatures may be higher but usually do not exceed the 1250°C. This limitation of working temperatures is one the main causes that make the conversion more heavy, for efficiency, compared to other conversion stages, shown in the figure 1.1, prevailing on

the overall performance of the entire conversion process.

Economic and system limits

In addition to the above limits, other ones have to be considered, of economic and system nature. For example in the thermal engines the more expansion of elastic fluid is pushed the greater is the global efficiency nevertheless, pushing the expansion over a certain point is uneconomical. An example is the Beau De Rochas cycle for internal combustion engines (see figure 1.3). In this cycle, expansion is interrupted in point 4. Giving up work that would be obtained by expansion to the point 4'. The extension of the expansion would increase the piston stroke and a consequent increase in the size of the engine (and costs) that can not be justified in economic terms.

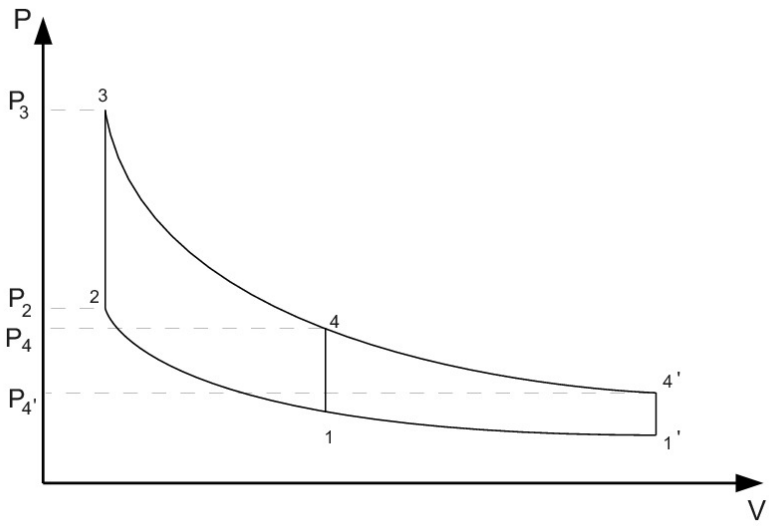

Figure 1.3: Beau De Rochas cycle for internal combustion engines

Similarly, in the generic cycle of a steam power plant (Hirn Cycle) one could reduce the pressure at the condenser (point 4, figure 1.4), to increase the steam expansion and then the work with the shaded area (4, 4', 5', 1", 1',

5=0). Nevertheless low pressure needs a low temperature, then a condenser with big size and too expensive in relation to the benefits obtained.

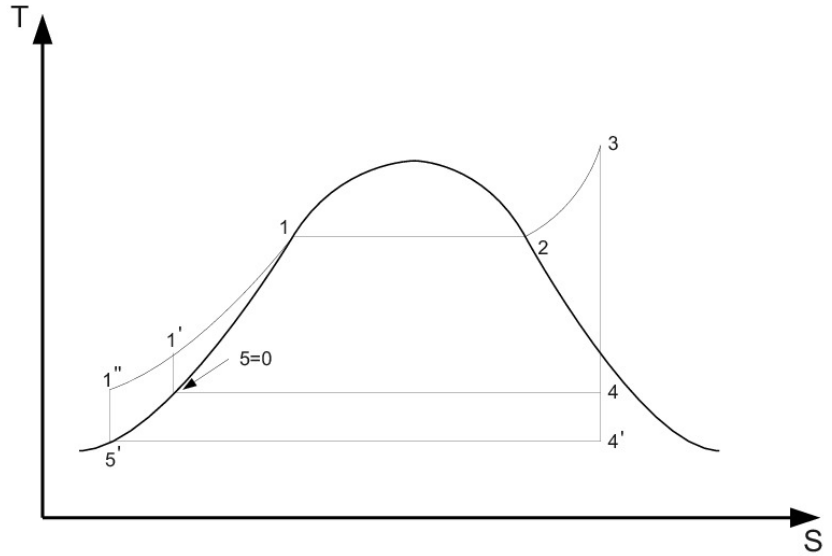

Figure 1.4: Hirn cycle for steam power plant

1.1.2 Main improvements in conversion systems

It was noted, therefore, that thermal engine plants operate at ranges temperature typically limited, so, for example, the steam engine plants have the maximum temperatures around 550°C, and in the gas turbine plants for generation around 1250°C . In the gas turbine the output temperature of the flue gas is also high (450°C to 650°C). This is therefore high enough to provide heat for a second cycle which uses steam as working fluid [11]. The systems, that work in the field of higher temperatures will be called "Topper", those that work in the field of lower temperatures will be called "Bottomer". Typical examples of the combined systems are consisting of a gas turbine (topper) and a steam power plant (bottomer). The heat input to the combined cycle is the same of the gas turbine, but the work output is greater (by the work of the Rankine cycle steam turbine). A schematic of the overall heat engine, which can be thought of as composed of an upper and a lower heat engine in series,

is given in figure 1.5. The upper engine is the gas turbine (Brayton cycle) which expels heat to the lower engine, the steam turbine (Rankine cycle).

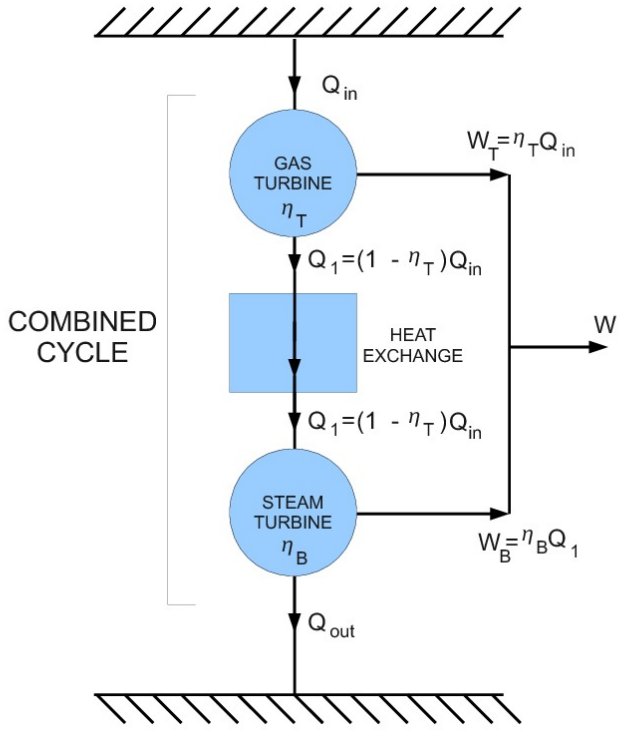

Figure 1.5: Schematic of combined cycle using gas turbine (Brayton cycle) and steam turbine (Rankine cycle)

The overall efficiency of the combined cycle can be derived as follows. We denote the heat received by the gas turbine as Q_{in} and the heat rejected to the atmosphere as Q_{out}. The hot exhaust gases from the gas turbine is used to generate steam by passing it through a heat exchanger with a live steam temperature between 420 and 580°C. This steam will be used to generate additional electricity via a steam turbine. In Topper converts the input energy Q_{in} with efficiency of η_T providing a useful amount of mechanical energy equal to $\eta_T Q_{in}$. If we assume that the remaining energy $(1-\eta_T)Q_{in}$ can be transferred entirely to the Bottomer system and that it will be converted with

efficiency of η_B it will provide a useful amount of mechanical energy equal to $\eta_B(1-\eta_T)Q_{in}$. Therefore, the total useful energy for a combined cycle is equal to

$$W = \eta_T Q_{in} + \eta_B(1-\eta_T)Q_{in} = (\eta_T + \eta_B - \eta_T\eta_B)Q_{in} \tag{1.2}$$

The ratio between the total work and the input heat Q_{in} is the global efficiency of the combined cycle:

$$\eta_{CC} = \frac{W}{Q_{in}} = \eta_T + \eta_B - \eta_T\eta_B \tag{1.3}$$

Equation 1.3 gives insight into why combined cycles are so successful. Let us suppose that the gas turbine cycle has an efficiency of 40%, which is a representative value for current Brayton cycle gas turbines, and the Rankine cycle has an efficiency of 30%. The combined cycle efficiency would be 58%, which is a very large increase over either of the two simple cycles. As one can see, the overall efficiency can also become very high. However, economic considerations, suggest the designer to choose a crossover between the fuel saving and to justify the additional costs resulting from the increased complexity of the combined cycle compared to the traditional ones.

1.2 Economic aspect of Power Generation

The total cost of a power generation plant or system should be as low as possible. This cost depends on three important factors: the capital cost, the fuel cost, and the operating costs. The capital cost is the price of the kilowatt installed, which depends on such factors as the expected lifetime of the station, the extent to which it is used, and its reliability. The fuel cost is directly related to the efficiency of the plant and the initial price of the raw fuel to be used. The operating and maintenance costs depend on the degree of simplicity and directness of the apparatus. Thus, it seems clear that efficiency alone is not always overriding criterion. A device of low efficiency but with low capital costs can compete under some circumstances. For instance, if the use of topper in a power plant is to be defendend, the total cost of the output kilowatt-hour for the conventional-topper plant should be larger than that of the plant alone. If c_T is the fixed cost per unit energy produced by the topper of efficiency η_T, c_B the cost produced by the conventional plant of efficiency

η_B and c_f is the fuel cost per unit heat input Q_{in} the total cost C_t of the output power from the conventional topper plant will be

$$C_t = Q_{in}c_B\eta_B + \frac{Q_{in}c_T\eta_T}{1-\eta_T} + \frac{Q_{in}c_f}{1-\eta_T}; \tag{1.4}$$

The first two terms on the right hand side of this equation represent the capital and operation costs of the conventional plant and the topper, respectively, whereas, the third therm represent the cost of the fuel. From figure 1.5 that show a combined cycle, it is seen that the total electric energy output is:

$$W = Q_{in}\eta_B + \frac{Q_{in}\eta_T}{1-\eta_T}; \tag{1.5}$$

Therefore, the cost c_T per unit energy output will be equal to the ratio of equation 1.4 to 1.5:

$$c_t = \frac{c_B\eta_B(1-\eta_T) + c_T\eta_T + c_f}{\eta_B(1-\eta_T) + \eta_T}; \tag{1.6}$$

For the topping to be economical, c_t should be smaller than the cost of the conventional plant alone:

$$c_t < c_B + c_f/\eta_B \tag{1.7}$$

This condition becomes

$$\frac{c_T}{c_B} < 1 + \frac{c_f(1-\tau_B)}{c_B\tau_B} \tag{1.8}$$

For modern power plants this ratio is slightly larger than two. Also note that this ratio is independent of the topping efficiency and it is only a function of the efficiency of the conventional power plant, the fuel cost per unit heat input, and the capital and operating costs of the conventional plant.

1.3 Direct energy conversion systems

As seen, the possibilities of improving significantly the conventional energy conversion processes are mainly related to technological progress. They still have small margins and for this reason the researchers have turned to

the development of other systems, so-called no-conventional. In the conventional conversion systems a significant loss of energy occurs, as mentioned, in the transition from thermal to mechanical energy (thermodynamic conversion). Research is focusing its efforts on conversion processes that do not use this step. The absence of moving mechanical parts, in particular, may allow the achievement of operating temperatures much higher than those typical of conventional processes, resulting therefore, at least potentially, a higher conversion efficiency. These processes are known as direct conversion, as primary and secondary energy is converted directly into electricity without the need to pass through a stage of mechanical energy [15]. The direct energy conversion methods that nowadays are taken into account in terms of industrial application are:

- Photovoltaic generation systems (Photovoltaic Solar Cells) [19] [7];
- Electrochemical energy conversion (Fuel Cells) [1];
- Magnetohydrodynamic generation(MHD) [4];
- Electrogasdynamic generation(EGD)[16];
- Thermoeletric power generation [2];

In the first two processes the conversion from the primary to the secondary energy form takes place avoiding the conversion in the intermediate thermal energy. The figure 1.6 shows the energy conversion stages in the direct generation of electric energy.

The design of an energy converter is often dictated by the type of energy to be converted, although it is the duty of the engineer to seek out new and more efficient ways of transforming the primary sources of the energy into electricity. There are many reasons for the use of new and direct conversion schemes. These can be grouped into three important areas: efficiency, reliability, and the use of new sources of energy. It is hoped that when a processes occurs directly, rather than passing through several steps, it is likely to be more efficient. This will lead to less expenditure of the primary energy reserve and a lower investment per installed unit power. Efficiencies are, however, still low at this stage of development of most direct energy conversion schemes. As for reliability, there are places where energy conversion equipment must run

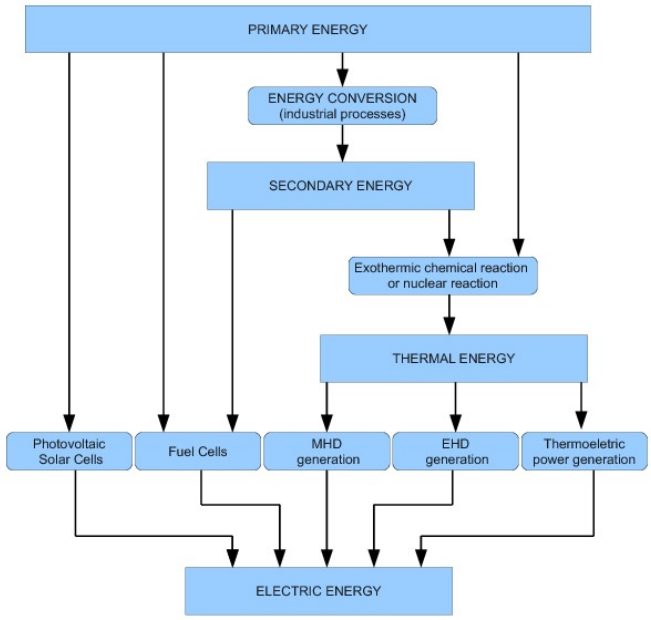

Figure 1.6: Direct energy conversion stages

for years without breaking down and without maintenance. These are situation where the ultimate reliability is required. Finally, the possibility of using new sources of energy seems enhanced by the development of the new direct energy converters.

There are many ways whereby the direct energy conversion of thermal to electrical energy can be obtained. In the following section the main one, magnetohydrodynamic power generation , is mentioned very briefly to give an overall background picture of the interest in direct conversion.

1.4 Magnetohydrodynamic power generation

The magnetohydrodynamic power generator [23] is a device that generates electric power by means of the interaction of a moving fluid (usually a ionized gas or plasma) and a magnetic field. As all direct conversion processes,

also the MHD generators can convert thermal energy directly into electricity without moving parts. In this way the static energy converters, with no moving mechanical part, can improve the dynamic conversion, working at temperature more higher than conventional processes. The typical configuration of MHD generator is shown in figure 1.7.

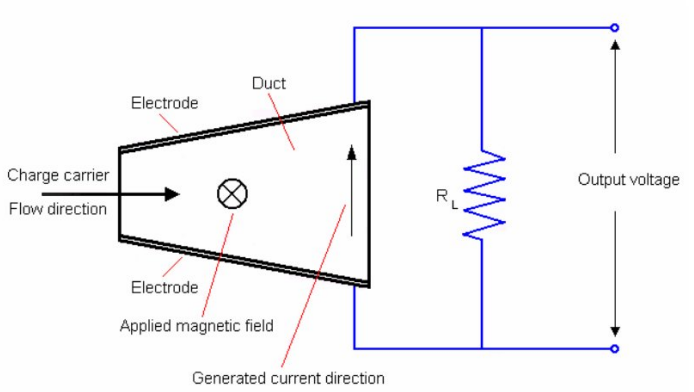

Figure 1.7: MHD channel

The underlying principle of MHD power generation is elegantly simple. Typically, an electrically conducting gas is produced at high pressure by combustion of a fossil fuel. The gas is then directed through a magnetic field, resulting due to the Hall effect. The MHD system constitutes a heat engine, involving an expansion of the gas from high to low pressure in a manner similar to that employed in a conventional gas turbogenerator. In the turbogenerator, the gas interacts with blade surfaces to drive the turbine and the attached electric generator. In the MHD system, the kinetic energy of the gas is converted directly to electric energy as it is allowed to expand.

It is known, that if we have a current flowing in a conductor immersed in a magnetic field, in the same conductor will be generated a Lorentz's force that is perpendicular to the direction of the magnetic field and to the current. The force can be expressed by the formula:

$$\vec{F} = q\vec{v} \times \vec{B} \tag{1.9}$$

where q is the electric charge moving with velocity $\vec{v}$ into a magnetic field

induction $\vec{B}$.

In an MHD converter the electrical conductor is replaced by a plasma current at high speed and with high temperature to be partially ionized [21]. So, the current flow is not only made of electrically neutral molecules but also with a mix of positive ions and electrons. When an high velocity gas flows into convergent-divergent duct and passes through the magnetic field an e.m.f is induced, mutual perpendicular to the magnetic field direction and to the direction of the gas flow. Electrodes in opposite side walls of the MHD flow channel provide an interface to an external circuit. Electrons pass from the fluid at one wall to an electrode, to an external load, to the electrode on the opposite wall, and then back to the fluid, completing a circuit. Thus the MHD channel flow is a direct current source that can be applied directly to an external load or can be linked with a power conditioning converter to produce alternating current. Of course, the electric energy produced is proportional to the reduction of kinetic energy and enthalpy of the fluid current. MHD effects can be produced with electrons in metallic liquids such as mercury and sodium or in hot gases containing ions and free electrons. In both cases, the electrons are highly mobile and move readily among the atoms and ions while local net charge neutrality is maintained. Any small volume of the fluid contains the same total positive charges in the ions and negative charges, because any charge imbalance would produce large electrostatic forces to restore the balance. Most theoretical and experimental work and power plant development and application studies have focussed on high-temperature ionized gas as the working fluid. Unfortunately, most common gases do not ionize significantly at temperatures obtainable with fossil fuel chemical reactions. This makes it necessary to seed the hot gasses with small amounts of ionizable materials such as alkali metals. Materials such as cesium and potassium have ionization potentials low enough that they ionize at temperatures obtainable with combustion reaction in air. Recovery and reuse of seed materials from the MHD channel exhaust are usually considered necessary from both economic and pollution standpoints.

Interest in MHD power generation was originally stimulated by the observation that the interaction of a plasma with a magnetic field could occur at much higher temperatures than were possible in a rotating mechanical turbine. The limiting performance from the point of view of efficiency of a heat engine is limited by the Carnot cycle. The efficiency of the Carnot cycle, which

establishes the maximum theoretical efficiency of a heat engine, is obtained by applying the equation 1.1. As shown in the figure 1.2, if the source temperature is $3000K$ and the sink temperature $300K$, the maximum theoretical efficiency would be 90%. Allowing for the inefficiencies introduced by finite heat transfer rates and component inefficiencies in real heat engines, a system employing an MHD generator offers the potential of an ultimate efficiency in the range of 60 to 65%. This is much better than the 35 to 40% efficiency that can be achieved in a modern conventional thermal power station [22].

The power output of an MHD generator for each cubic metre of its channel volume is proportional to the product of the gas conductivity, the square of the gas velocity, and the square of the strength of the magnetic field through which the gas passes. For MHD generators to operate competitively with good performance and reasonable physical dimensions, the electrical conductivity of the plasma must be in a temperature range above about $1800K$.

Apart of the MHD power generator, other apparatus are necessary to form the overall MHD system. It is necessary to burn the fuel and the oxidizer, to add the seed, and to make arrangements for exporting the generated electrical power. The fuel is usually fossil and the oxidizer is air, for obvious economic reasons. For large systems, some precautions should be taken to limit the amount of losses. The air may be enriched with more oxygen, and preheating of the incoming oxidizer becomes necessary to allow thermal ionization. In practice a number of issues must be considered in the implementation of a MHD generator: Generator efficiency, Economics, and Toxic products. These issues are affected by the choice of one of the three MHD generator designs. These are the Faraday generator, the Hall generator, and the disk generator [20].

A simple Faraday generator would consist of a wedge-shaped pipe or tube of some non-conductive material. When an electrically conductive fluid flows through the tube, in the presence of a significant perpendicular magnetic field, a charge is induced in the field, which can be drawn off as electrical power by placing the electrodes on the sides at 90 degree angles to the magnetic field. The main practical problem of a Faraday generator is that differential voltages and currents in the fluid short through the electrodes on the sides of the duct. The most powerful waste is from the Hall effect current.

The most common answer is to use the Hall effect to create a current that flows with the fluid. The normal scheme is to place arrays of short, vertical

electrodes on the sides of the duct. The first and last electrodes in the duct supply the load. Each other electrode is shorted to an electrode on the opposite side of the duct. Losses are less than that of a Faraday generator, and voltages are higher because there is less shorting of the final induced current. However, this design has problems because the speed of the material flow requires the middle electrodes to be offset to 'catch' the Faraday currents. As the load varies, the fluid flow speed varies, misaligning the Faraday current with its intended electrodes, and making the generator's efficiency very sensitive to its load.

The third, currently most efficient answer is the Hall effect disk generator. This design currently holds the efficiency and energy density records for MHD generation. A disk generator has fluid flowing between the center of a disk, and a duct wrapped around the edge. The magnetic excitation field is made by a pair of circular Helmholtz coils above and below the disk. The Faraday currents flow in a perfect dead short around the periphery of the disk. The Hall effect currents flow between ring electrodes near the center and ring electrodes near the periphery. Another significant advantage of this design is that the magnet is more efficient. First, it has simple parallel field lines. Second, because the fluid is processed in a disk, the magnet can be closer to the fluid, and magnetic field strengths increase as the 7th power of distance. Finally, the generator is compact for its power, so the magnet is also smaller. The resulting magnet uses a much smaller percentage of the generated power.

As of 1994, the 22% efficiency record for closed-cycle disk MHD generators was held by Tokyo Technical Institute. Typical open-cycle Hall duct coal MHD generators are lower, near 17%. These efficiencies make MHD unattractive, by itself, for utility power generation, since conventional Rankine cycle power plants easily reach 40%.

However, the exhaust of an MHD generator burning fossil fuel is almost as hot as the flame of a conventional steam boiler. By routing its exhaust gases into a boiler to make steam, MHD and a steam Rankine cycle can convert fossil fuels into electricity with an estimated efficiency up to 60 percent, compared to the 40 percent of a typical coal plant. Retrofitting and/or repowering of existing thermal power plants is possible with a significant increase of the efficiency of the plant. Efficiencies greater than 65-70% can be reached if a triple cycle, including an MHD generator, a gas turbine and a steam turbine, is utilized. The abundance of coal reserves throughout much of the world has

favoured the development of coal-fired MHD systems for electric power production. Coal can be burned at a temperature high enough to provide thermal ionization. However, as the gas expands along the duct or channel, its electrical conductivity drops along with its temperature. Thus, power production with thermal ionization is essentially finished when the temperature falls to about 2,500 K (about 2,200°C, or 4,000°F). To be economically competitive, a coal-fired power station would have to combine an MHD generator with a conventional steam plant in what is termed a binary cycle. The hot gas is first passed through the MHD generator (a process known as topping) and then onto the turbogenerator of a conventional steam plant (the bottoming phase). An MHD power plant employing such an arrangement is known as an open-cycle [13], or once-through, system. The figure 1.8 shows the typical open cycle scheme for a coal-fired MHD systems for electric power production [12].

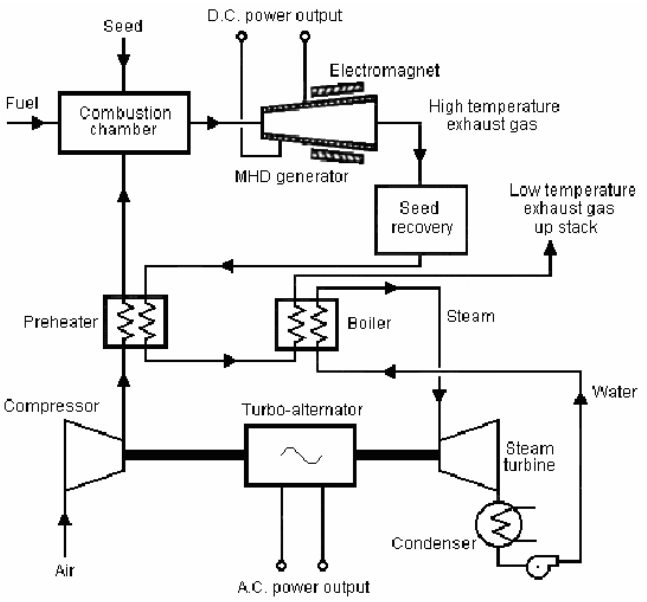

Figure 1.8: The typical open cycle scheme for a coal-fired MHD systems

Coal combustion as a source of heat has several advantages. For example, it results in coal slag, which under magnetohydrodynamic conditions is molten and provides a layer that covers all of the insulator and electrode walls.

The electrical conductivity of this layer is sufficient to provide conduction between the gas and the electrode structure but not so high as to cause significant leakage of electric currents and consequent power loss. The reduction in thermal losses to the walls because of the slag layer more than compensates for any electrical losses arising from its presence. However, the dust could degrade the MHD generator elements. In fact, an important item in the development of the MHD generator is the development of a durable electrode. The development of suitable materials for use in mhd generator is one of the most challenging areas. The very high temperatures (2700 K) coupled with the highly corrosive seed-laden atmosphere limit the choice of materials in contact with the plasma. These materials in contact with the high temperature plasmas in mhd generator are simultaneously subjected to stresses of mechanical, thermal, chemical and electromagnetic nature. The use of a seed material in conjunction with coal offers environmental benefits. In particular, the recombination chemistry that occurs in the duct of an MHD generator favours the formation of potassium sulfate in the combustion of high-sulfur coals, thereby reducing sulfur dioxide emissions to the atmosphere. The need to recover seed material also ensures that a high level of particulate removal is built into an MHD coal-fired plant. Finally, by careful design of the boiler and the combustion controls, low levels of nitrogen oxide emissions can be achieved. The problems due to the direct combustion of coal can be overcome combining the MHD generator on the Integrated Gasification Combined Cycle (IGCC). it is a technology that turns coal into gas synthesis gas (syngas). All the treatments on the gas are performed before the combustion, so that the electrostatic precipitator is no longer necessary. On the other hand, eliminating the most part of the sulfur before the Claus/Scot process is a great advantage, in particular in the cases of coal with a high percentage of sulfur. In addition to natural gas as a fuel source, more MHD power generation systems have been proposed. A magnetohydrodynamic generator might be heated by a Nuclear reactor (either fission or fusion). Reactors of this type operate at temperatures as high as 2000°C. By pumping the reactor coolant into a magnetohydrodynamic generator before a traditional heat exchanger an estimated efficiency of 60% can be realised. The figure 1.9 shown the typical close-cycle system for nuclear source [24].

In theory, solar concentrators can provide thermal energy at a temperature high enough to provide thermal ionization. Thus, solar-based MHD sys-

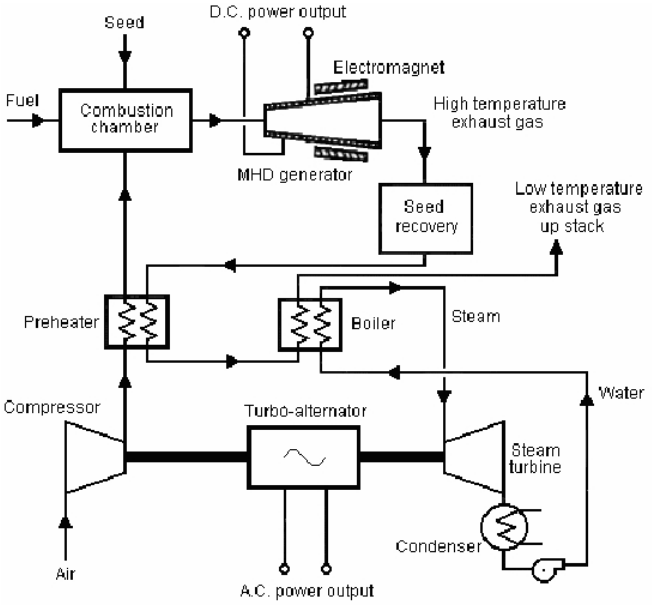

Figure 1.9: The typical close cycle scheme for nuclear source

tems [25] have potential, provided that solar collectors can be developed that operate reliably for extended periods at high temperatures. MHD generators have not been employed for large scale mass energy conversion because other techniques with comparable efficiency have a lower lifecycle investment cost. Advances in natural gas turbines achieved similar thermal efficiencies at lower costs, by having the turbine's exhaust drive a Rankine cycle steam plant. To get more electricity from coal, it is cheaper to simply add more low-temperature steam-generating capacity. Presently, the most often considered use if MHD generator is as a topping device for conventional steam plants. The fact there are no moving mechanical parts will make operation at high temperature feasible. The upper limit temperature in a steam plant is about 750°C, which is far below the temperatures reached by MHD generators (about 2700°C). To obtain good conducting gases, it is necessary to add cesium or potassium as seed materials and to solve the problem of corrosion. Advances in refractory material are needed. The cost of seeding increases substantially the cost of installed power. The cost of wall material is an important part of the total cost

of an MHD generator. Good insulating and refractory materials working for a reasonably long time without deterioration should be found. The problem of high temperatures could be alleviated by the use of some type of nonthermal ionization. This can also make the possibility of a nuclear reactor MHD generator coupling feasible, with the advantage of having an entirely static power plant. From the tremendous amount of work done in this field, both theoretically and experimentally, it seems that a fossil fueled MHD topper is the most promising MHD generator and most probably will be the first to be operating to on the industrial level. Many problems need to be solved before an MHD power plant becomes competitive: seed recovery, superconductivity for the magnet, high temperature materials, AC power generation, and progress in non equilibrium ionization techniques.

Chapter 2

Physical principles

Before treating the following chapters it will be hopeful to review the important physics principles. This chapter is divided into two parts: thermodynamics, and Plasma physics.

2.1 Heat and work [28] [8]

It is well know that when two systems at different temperatures are placed togheter, both will reach a final temperature which is between the initial temperature of the two systems. It is know that heat has been transferred from one system to the other. It can be said that heat is what is transferred between a system and the world outside (of the system) as a results of temperature difference only. As a result, heat can be measured, and a unit of heat can be defined as the heat necessary for the production of a standard change in temperature. One of the important unit of heat is the calorie. One calorie (cal) is the quantity of heat necessary to raise the temperature of 1 g of water from 14.5°C to 15.5°C. The heat capacity C is an important characteristic of body. It is defined as the ratio of the quantity of heat ΔQ supplied to a body to its corresponding temperature rise ΔT, or in the limit $C = \delta Q/\delta T$. The specific heat c_M is the heat capacity per unit mass M:

$$c_M \gamma = C/M \tag{2.1}$$

the specific heat of a material has a unique value only when the conditions of volume and pressure are specified. At constant pressure p_r the unique value of $c_M\gamma$ is

$$c_p = \frac{1}{M}\frac{\delta Q}{dT}\Big]_{p_r} \tag{2.2}$$

and a constant volume V it is

$$c_v = \frac{1}{M}\frac{\delta Q}{dT}\Big]_{V} \tag{2.3}$$

Heat can also be defined as energy flowing from one system to another because of a temperature difference between the two systems. The energy transmitted without affecting the temperatures is defined as work W. Both Q and W are associated with the interaction between the system and the surrounding environment. If the system is a gas in a cylindrical container with a movable piston, where the gas under pressure works on a piston by exerting a force and producing a displacement of the piston as shown in figure 2.1, Q and W can be computed for a specific thermodynamic process. The gas at pressure p_r

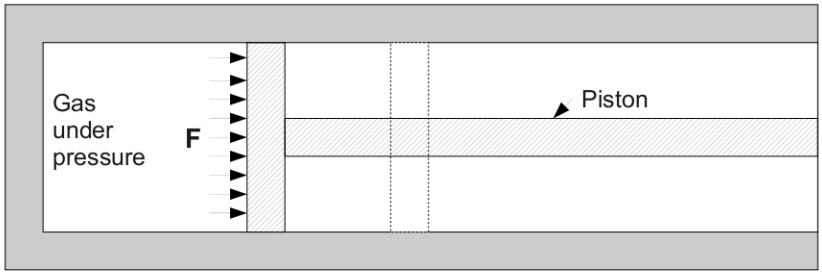

Figure 2.1: Cylindrical container with a movable piston and a gas under pressure

does work δW in the piston of surface area S by exerting a force $F = p_r S$ and producing a displacement ds. The amount of this work is $\delta W = Fds$, or

$$\delta W = p_r dW \tag{2.4}$$

where V is the volume of gas. The total work W done by the system on the piston is

$$W = \int_{V_i}^{V_f} p_r dV \tag{2.5}$$

where V_i stands for initial volume and V_f stands for final volume as show in the figure 2.2. There are many ways in which the system can be taken from

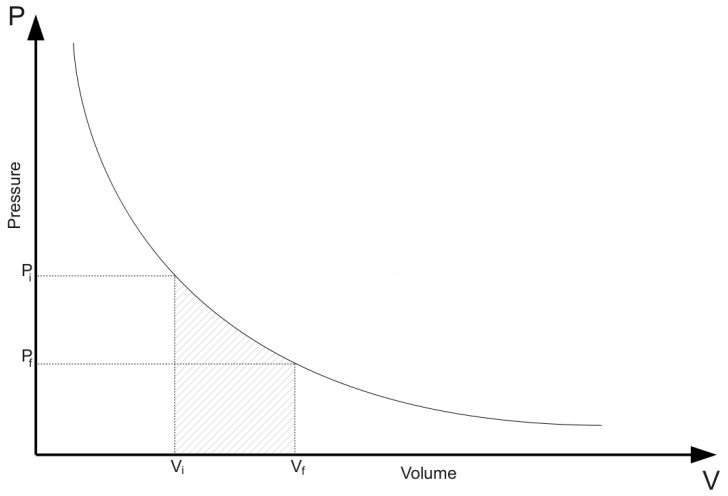

Figure 2.2: P-V diagram where the work done by the system is represented by the shaded area

the initial state to the final state. It can be seen that the work done by a system depends on both the initial and final states end on the path between these states the same can be said about the heat lost or gained by the system.

2.1.1 The first law of thermodynamics

The first law of thermodynamics is an expression of the principle of conservation of energy. It states that energy can be transformed (changed from one form to another), but cannot be created or destroyed. The first law of thermodynamics says that energy is conserved in any process involving a thermo-

dynamic system and its surroundings. A system that is in contact with other systems loses energy to, or gains energy from, the other systems. When a system has its state changed from S_i to S_f by following different paths, it is found that the difference $Q - W$ is always the same, independent of the path followed. This difference depends only on the initial and final states and is defined as the internal energy function U. It represent the internal energy change of the system. From the principle of conversation of energy,

$$dU = \delta Q - \delta W \tag{2.6}$$

where δQ and δW are infinitesimal amount of heat supplied to the system and work done by the system, respectively. A process is called *adiabatic* when the change of state is accomplished without any transfer of heat ($\delta Q = 0$). An adiabatic process in which no work is performed on or by the system is called a *free expansion process* ($\delta Q = \delta W = \delta U = 0$).

2.1.2 Kinetic theory of gases

It is well know that all gases can be approximated by an ideal gas model if their density is not too high. An ideal gas can be described by the equation of state

$$PV = nRT \tag{2.7}$$

where

- P is the pressure;
- V is the volume;
- n is the amount of substance of the gas (in moles);
- T is the absolute temperature;

This equation represent the macroscopic state of an ideal gas. Microscopically, an ideal gas is assumed to be in random motion, obeying Newton's laws of motion. The relationships between the macroscopic characteristics and the macroscopic quantities P, V, and T can be found. It is found that $P = \frac{1}{2}Mn\upsilon^2$ where M is the molecular mass and υ is the particle mean square velocity. By

taking into consideration the equation of state, the total translational kinetic energy of the gas molecules is found to be directly proportional to the absolute temperature T:

$$T = \frac{\frac{1}{2}Mv^2}{\frac{3}{2}k} \tag{2.8}$$

where k is the Boltzmann constant ,$k = \frac{Rn}{N} = \frac{R}{k} = 1.38 \times 10^{-23} J/^\circ K$, where N is the total number of molecules $N = nV$ and N_0 is the Avogadro's number, $N_0 = \frac{N}{n} = \frac{R}{k} = 6.023 \times 10^{23}$ molecules/mole. The equation of state can be written $PV = NkT$. The internal energy of a ideal gas is found to depend only on temperature, $U = \frac{3}{2}NkT$.

2.1.3 The Carnot cycle

In a simple heat engine, heat is extracted from a heat source at one temperature and rejected to another source at a lower temperature, with a useful work output. In figure 2.3, the heat Q_h from the boiler, which is at temperature T_h, is transferred to a heat engine, and heat Q_c is transferred from the engine to the radiator, which is at a lower temperature T_c. For an engine to operate indefinitely, it should return to its initial state periodically after following a certain cycle. Consider the system of figure 2.3; from the first law ($dU = 0$).

$$W = Q_h - Q_c \tag{2.9}$$

where Q_h is the heat from the boiler, with temperature T_h, transferred to a heat engine, and then, Q_c is the heat transferred from the engine to the radiator, which is at a lower temperature T_c. The thermal efficiency η is the ratio of the output to the input. Thus $\eta = W/Q_h$ and introducing 2.9,

$$\eta = 1 - \frac{Q_c}{Q_h} \tag{2.10}$$

Increasing Q_h and decreasing Q_c results in a more efficient engine. There are an infinite variety of possible cycles and many different kinds are utilized for engines. A particular important one is the Carnot cycle. This is an idealized cycle for converting heat into mechanical energy, and it is illustrated by the $p-V$ diagram of figure 2.4 for the case of a gas. The cycle is composed of four

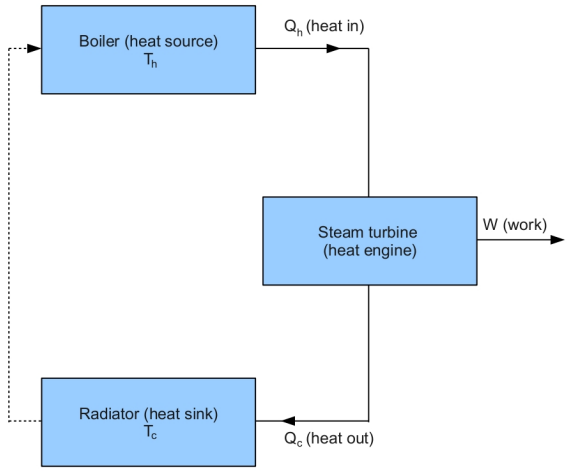

Figure 2.3: Example of a heat engine

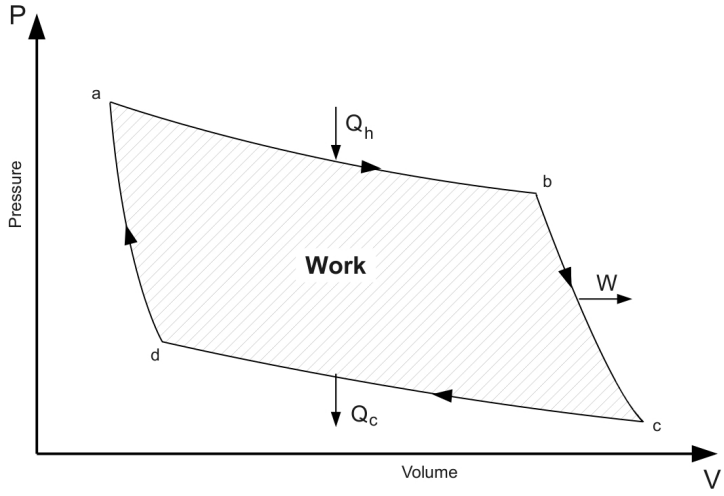

Figure 2.4: P-V diagram of a Carnot cycle of a gas

paths delineated by the intersection of a pair of adiabatics ($Q = costant$) and a pair of isotherms (T=constant).

1. Path a-b: *isothermal expansion at high temperature T_h;*
2. Path b-c: *adiabatic expansion;*
3. Path c-d: *isothermal compression at low temperature T_c;*
4. Path d-a: *adiabatic compression.*

For an ideal gas subjected to the Carnot cycle, it is easy to show that $Q_h/T_h = Q_c/T_c$, and that from equation 2.10 the Carnot efficiency is $\eta_c = 1 - T_c/T_h$, where the temperature are in Kelvin. It can be shown that for any real engine operating between T_h and T_c, the efficiency cannot exceed the carnot efficiency, and always $\eta \leq \eta_c$. This is a serious limitation on efficiency, since T_c can never reach $0K$ and T_h is limited by obvious technological problems.

2.2 Basic Elements of Plasma Physics [10] [18]

Plasma is a state of the matter similar to gas, in which a part of molecules are ionized. Usually the plasmas are subdivided into several typologies, depending on the temperature level. The behavior of the plasma is rather different from that of neutral fluid, because electromagnetic forces affect the dynamics of the particles. For increasing values of temperature, the matter firstly passes from a solid to a liquid state, then to a neutral gas and then to a rising degree of ionization. Depending on such ionization degree we will speak of cold plasma, thermonuclear plasma and fusion plasma. In a plasma, the kinetic energy of electrons and ions is greater than the atomic ionization potential, and for that it can subsist in equilibrium conditions. In such condition the equilibrium is described by the Saha equation:

$$\frac{n_e n_i}{n_n} = \frac{(2\pi m_e kT)^{3/2}}{h^3} exp\left(-\frac{U_i}{kT}\right); \tag{2.11}$$

where

- n_i = number of ions per m^3;
- m_e = electron mass;

- n_e = electron concentration per m^3;
- n_n = number of neutral particles per m^3;
- k =$1.38 \cdot 10^{23} J/K$ in the Boltzmann constant;
- T= temperature in K;
- U_i = ionization energy of the gas;

The presence in the gas of both positive and negative charged particles makes the dynamic behavior of the gas rather different with respect to a non ionized gas, due to the presence of long range forces. For this reason it is not proper to take into account only collisions when one consider the interaction among particles. On the contrary, sometimes the collisions can be neglected on first approximation, the dynamic being well described only considering electric and magnetic interactions.

In plasma, the ionization a dynamic process that takes place when the kinetic energy of particles is greater than the ionization energy χ_1 which represents a threshold value. For a given temperature, one has the equilibrium ionization, where the rate of ionization is equal to the rate with which free electrons are captured by ions (recombination). In figure 2.5 the behavior of the ionization of the atomic hydrogen is given. The ionization rate has a maximum when the specific energy is 10 times the ionization energy χ_1, but as the temperature increases the recombination rate decreases, so that the ions concentration becomes more and more greater as the temperature increases. At room temperature the ionization is negligible.

The two independent characteristics of a plasma are the charged particle density n and the temperature T. Since the plasma is in the average neutral, the positive charge particle number concentration n_p equals the negatively charged particle number concentration n_e. When the plasma departs from neutrality , $\delta n = n_p - n_e$ is defined. Two other characteristics are important for the description of a plasma. There are the Debye radius r_D and the characteristic plasma frequency ω_p. The Debye radius is defined as the radius of a sphere concentric to the charged particle such that at its surface, the kinetic energy $2\gamma kT$ of the particles equals eV, where V is the potential. By solving Poisson's equation law in spherical cordinates and considering only the effect of the electron ($\Delta n = -n_e$), the Debye radius is found to be equal to

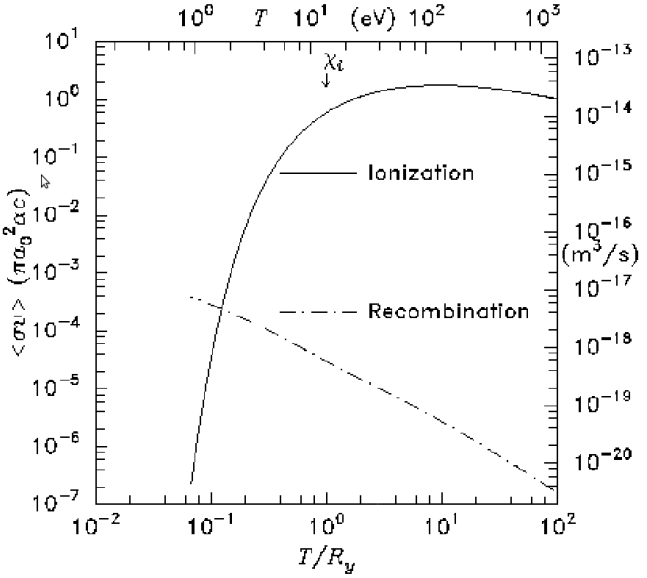

Figure 2.5: Ionization recombination diagram

$$r_D = \sqrt{\frac{\varepsilon kT}{e^2 n_e}} \tag{2.12}$$

To calculate the characteristic plasma frequency, consider a plasma region of thickness l and displacement of all electrons at distance x. The heavy ions can be disregarded, since the light electron will react much more quickly. The balance of forces requires that at equilibrium the force due to the electron field E be equal to Newton's force due to the acceleration. After using Poisson's law to replace E, a wave equation in x is obtained:

$$x + \frac{M\varepsilon_0}{n_e e^2}\frac{d^2x}{dt^2} = 0 \tag{2.13}$$

The solution is $x = x_0 exp(j\omega_p t)$ where ω_p is the characteristic plasma frequency for the electrons; it is equal to

$$\omega_p = \sqrt{\frac{en}{M\varepsilon}} \tag{2.14}$$

The plasma will then oscillate with a frequency $f_p = \omega_p/2\pi$ around its steady state position. A plasma can not exist without charge separation, which takes place if the collision effects are dominant compared to single particle effects. The second for existence of a plasma is that on the average the ionized gas should remain neutral. In order that oscillations may develop in a plasma, the collisional damping frequency ν_c should satisfy $\omega_p \gg \nu_c$.

2.2.1 Temperature and Pressure of the Plasma

The pressure of a gas contained in a vessel is given by the relation of Bernoulli:

$$P = \frac{2}{3}\rho\left(\frac{1}{2}mv^2\right); \tag{2.15}$$

Where m and v are respectively the mass and the velocity of the generic particle. In a mono-dimensional gas in thermal equilibrium, the particles velocities follow a Maxwellian distribution:

$$f(u) = A \cdot e^{\frac{1mv^2}{2kT}}; \tag{2.16}$$

where n is the total concentration of particles. This is related to the distribution $f(u)$ by the following:

$$n = \int_{-\infty}^{\infty} f(u)du; \tag{2.17}$$

The average kinetic energy is given by:

$$E_{av} = \frac{\int_{-\infty}^{\infty} \frac{1}{2}mu^2 f(u)du}{\int_{-\infty}^{\infty} f(u)du} \tag{2.18}$$

By defining $v_{th} = \sqrt{(2kT/m)}$ and $y = u/v_{th}$, the previous relation can be expressed as:

$$E_{av} = \frac{\frac{1}{2}mAv_{th}^3 \int_{-\infty}^{\infty} e^{-y^2} \cdot y^2 dy}{Av_{th}\int_{-\infty}^{\infty} e^{-y^2} dy} \tag{2.19}$$

By solving by parts the numerator, one obtain the following relation valid for a mono-dimensional flow:

$$E_{av} = \frac{1}{2}kT \tag{2.20}$$

It is possible to demonstrate that in case of three-dimensional distribution of velocities, the previous relation becomes

$$E_{av} = \frac{3}{2}kT \tag{2.21}$$

2.2.2 Unbalanced plasma

Let us consider a ionized gas which in a particular region or instant has a different number of positive and negative charges. To fix the ideas, we will consider the case of mono-atomic hydrogen. In said region or instant, one will have a charge density equal to:

$$\rho = n_e(-e) + n_i(+e) = e(n_i - n_e) \tag{2.22}$$

The electric field due to the unbalanced charges gives rise to a repulsive force that tends to throw out said charges and to re-establish the neutrality of the gas. Such force is some order of magnitude greater than that due to the pressure, therefore the interaction of charges carries with neutral particles cannot reach the equilibrium with repulsive forces between charges of the same sign, but anyway they can affect the dynamic behavior of charges carries. In the presence of an external electric field, applied to the plasma by means of the plates of a capacitor, the charges carries migrate toward the plate of opposite sign forming two clouds of charge, until the total field in the plasma is null. The depth of the layer is given by the Debye's length.

2.2.3 Length of Debye

The length of Debye is one of the most important parameters which characterize a plasma. In order to defining it, let us assume the distribution be mono-dimensioal. Let Φ be the potential in the position $x = 0$. Let us further assume that the mobility of electrons is much greater than that of ions. From Poisson's equation derives:

$$\varepsilon_0 \frac{d^2\Phi}{dx^2} = -e(n_i - n_e) \tag{2.23}$$

The distribution of velocities of a ionized gas, where a potential is present, is given by the Boltzmann's equation:

$$f(u) = A \cdot e^{\frac{(1/2)mu^2 + q\Phi}{kT}} \tag{2.24}$$

By integrating for $\Phi \to 0$ with boundary conditions: $n_e = n_i$ and $n_e = n_\infty$ one obtains :

$$n_e = n_\infty e^{\frac{e\Phi}{kT}} \tag{2.25}$$

By substituting this expression in the Poisson's equation we obtain:

$$\varepsilon_0 \frac{d^2\Phi}{dx^2} = e n_\infty \left(e^{\frac{e\Phi}{kT}} - 1 \right) = e n_\infty \left[\frac{e\Phi}{kT} + \frac{1}{2} \left(\frac{e\Phi}{kT} \right)^2 + ... \right] = e n_\infty \frac{e\Phi}{kT} \tag{2.26}$$

By defining $\lambda_D = \sqrt{\frac{\varepsilon_0 kT}{ne^2}}$ (length Debye), we can obtain the trend of the potential:

$$\Phi = \Phi_0 \cdot e^{-|x|/\lambda_D} \tag{2.27}$$

The length of Debye gives us the dimension of the layer of charges, which is related to the action radius of Coulombian interactions in the plasma. The most influencing parameter of plasma results to be the electrons concentration, as the mobility of the ions is rather lower.

2.2.4 Gas conductivity

A gas, to be utilized as a working fluid, should be sufficiently conducting, therefore, ionized. Ionization is a process in which electrons are removed from atom. Conductivity is due to the free electrons and positive ions which move under the effect of electric field. The electrical conductivity of an ionized gas may be calculated approximately by considering the current density $\vec{J}$ resulting from an applied electric field $\vec{E}$.

$$\vec{J} = \sigma \vec{E} \tag{2.28}$$

the current density can also be defined as a function of velocity of ions which move under the effect of the electric field.

$$\vec{J} = nev \tag{2.29}$$

where n is the number concentration of ions or electrons, e is the electronic charge, and v is the velocity of the electrons. The mobility b is defined by:

$$v = b\vec{E} \tag{2.30}$$

Introducing equation 2.30 into 2.29 and comparing 2.28 and 2.29 yields

$$\sigma = neb \tag{2.31}$$

In the absence of an electric field, the paths of the particles are straight lines disturbed only after collisions, in a random manner. The effect of the electric field is to create a drift velocity of the particles in the direction of the field after each collision. If τ is the average collision time of a particular electron, the increase of its mean relative velocity will be from zero to $(eE\tau/M)$. Therefore, the average velocity will be $\bar{v} = eE\tau/2M$ and the mobility will be $b = e\tau/2M$. Replacing b by its value in equation 2.31 We have:

$$\sigma = \frac{1}{2} ne^2 \tau / M \tag{2.32}$$

Taking into account the fact that there is a random distribution about the mean collision time τ, the coefficient $1/2$ should be replaced by a more general factor l_λ. It is also practical to use the collision frequency ν_c instead of τ, then ν_c is defined as $\nu_c = 1/\tau$ and equation 2.32 becomes

$$\sigma = \frac{l_\lambda ne^2}{M\nu_c} \tag{2.33}$$

In their motion under the effect of the electric field, the electrons may collide with any type particle existing in the plasma, such as electrons, ions, and neutral particles. The effect of electron- electron collisions can be neglected, since they will not change the average energy of the electrons in an appreciable manner. If ν_{en} and ν_{ei} are the collision frequencies of the electron with the neutral particles and the ions, respectively, the total collision frequency can be written $\nu_c = \nu_{en} + \nu_{ei}$. Replacing ν_c by its value in equation 2.33, it is found that $1/\sigma = 1/\sigma_{en} + 1/\sigma_{ei}$, where σ_{en} and σ_{ei} are the electron-neutral particle and electron-ion conductivities, respectively

$$\sigma = \frac{l_\lambda ne^2}{M\nu_{en}} \tag{2.34}$$

$$\sigma = \frac{l_\lambda n e^2}{M \nu_{ei}} \tag{2.35}$$

the collision frequencies are related to the collision cross sections Q_{en} of electrons with neutral particles, and Q_{ei} of electron with ions, according to the relations

$$\nu_{en} = n_n \bar{v} Q_{en} \tag{2.36}$$

and

$$\nu_{en} = n_i \bar{v} Q_{ei} \tag{2.37}$$

If a magnetic field is applied, the electrons will drift in a direction influenced by the magnetic field and not necessarily parallel to the electric field. Under these conditions the electrical conductivity becomes a tensor. On the other hand, since the Hall parameter for ions is smaller than that for electrons, due to their higher ionic mass, the ion current is not as greatly affected by the presence of the magnetic field. As the magnetic field is increased, the electron current decreases to the point where it becomes of the same order of magnitude as the ionic current. This phenomenon is called ion slip, and arrangements should be taken to avoid it.

There are several type of ionization:

- Thermal ionization;
- Magnetically induced ionization;
- Radio-frequency wave induced ionization;
- Radioactivity;
- Photoionization;
- Electron-beam ionization;
- Flames;

Thermal ionization

The thermal ionization is the most important method of ionizing a plasma. In this case, ionization is obtained by giving enough thermal energy to the gas. Considering a gas in thermodynamic equilibrium at a temperature T, the equilibrium of the ionization reaction, $A \Leftrightarrow A^+ + e$ can be calculated by using statistical mechanical principles. This has been done by Saha leading to his famous equation

$$\frac{n_e n_i}{n_n} = 2\frac{P_i}{P_n}\left(\frac{2\pi MkT}{h^2}\right)^{3/2} exp\left(-\frac{eV_i}{kT}\right) \tag{2.38}$$

where n_e, n_i, and n_n are the electron, ion, and neutral particle densities, P_i and P_n are the internal partition functions for the ion and the neutral particles, respectively, and V_i is the ionization potential of the gas. If it is assumed that the plasma is, on the average, neutral and only partially ionized, then $n_e = n_i \ll n_n$. Introducing this in the equation 2.38, we get

$$n_e = \left(\frac{2n_n P_i}{P_n}\right)^{1/2}\left(\frac{2\pi MkT}{h^2}\right)^{3/2} exp\left(-\frac{\frac{1}{2}eV_i}{kT}\right) \tag{2.39}$$

and by replacing n_e by its value in equations 2.34 and 2.35, one can obtain the expression for the conductivities. Note here that the conductivity is inversely proportional to the square root of the gas density n_n. The ration (P_i/P_n) depends on the nature of the material and on the temperature. To have a large value of σ, n_e should be large. From equation 2.39, it follows that the degree of ionization will be much large for small values of the ionization potential. The ionization potential of the air, combustion gases, and noble gases used for direct conversion generators, as MHD generator and EHD generator, is usually very high. This fact led to the necessary of seeding the gas with material with a low V_i such as cesium or potassium.

2.2.5 Force between charge carries

There are two important classes of intermolecular forces: short-range forces and long-range forces. Short-range forces are repulsive because the atoms are so close to each other that their clouds overlap. Long-range forces such as those due to electrostatic, inductive, and dispersive effects are attractive.

Many mathematical models have been proposed to the description of the long-range potential. A simple realistic model is deduced from the hard sphere suggestion in which the potential is assumed equal to zero outside the hard molecule and becomes infinite at its surface. A more realistic model has been proposed by Lennard-Jones and it is widely used.

$$eV(r) = 4\epsilon_r = 4\epsilon_m[(r_m/r)^{12} - (r_m/r)^6] \tag{2.40}$$

This is shown in figure 2.6. ϵ_m is the maximum energy of attraction which

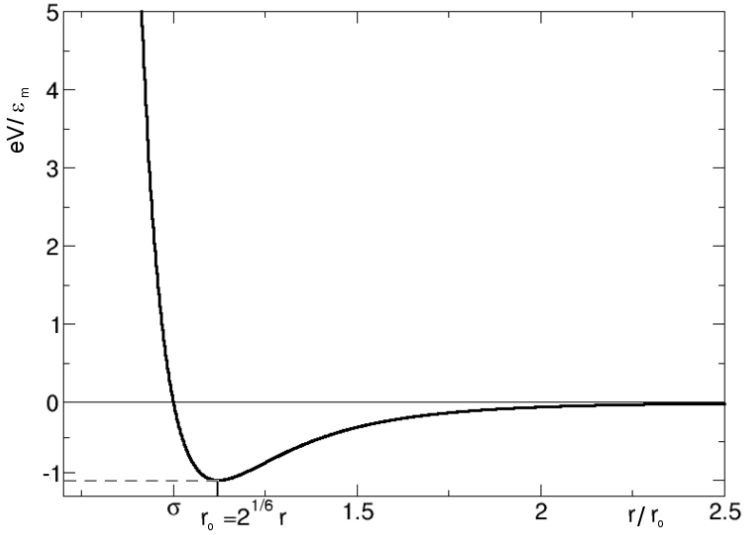

Figure 2.6: The Leonnard-Jones potential.

occurs at $r_0 = 2^{1/6} r_m$. This equation for most spherical nonpolar molecules, r is the distance between the particles, and r_m s the distance at which the potential reaches its minimum. In the presence of an electric field $\vec{E}$, the force $\vec{F}$ acting on a medium of charge density ρ_e is $F = \rho_e \vec{E}$, and in the presence of an electromagnetic field, the Lorenz force is

$$\vec{F} = \vec{J} \times \vec{B} + \rho_e \vec{E} \tag{2.41}$$

2.2.6 Boltzmann equation

In describing the behaviour of a plasma, which necessarily consists of a large number of particles, a statistical approach is used. This approach, known as classical statistics, is based on the laws of classical mechanics. It is valid only for systems in which the total volume is much larger than the individual volume of particle. If the effect of collision is considered, the well known Boltzmann's equation is found readily:

$$\frac{\partial f_e}{\partial t} + v\frac{\partial f_e}{\partial r} + \frac{\vec{F}}{M}\frac{\partial f_e}{\partial v} = \frac{\partial f_e}{\partial t} \tag{2.42}$$

The velocity distribution function f_e gives the probability that a particle of velocity v and the coordinate $\vec{r}$ be in the phase space. The left-hand side of the equation is the drift term and the right-hand is the collision term. The force acting on the particle is $F(\vec{r}, t)$. Boltzmann equation is valid for each type of plasma particle separately. It is very important, since all the transport coefficients can be deduced directly from it. When the force is due to an electromagnetic field, its value becomes $\vec{F} = e(\vec{E} + v \times \vec{B})$.

2.2.7 Transport phenomena

In the absence of any external force, the random motion of the plasma particle will result in a particle current from one region to another only if there exist gradients of particle density, pressure, or temperature in the plasma. The next effect of an applied external force is to cause the particles to move in a direction determined by the force. The existence of such motion results in mass and charge transports which are the most elementary of the transport phenomena. These phenomena are simply described by five transport coefficients: diffusion D, mobility b, electrical conductivity σ, thermal conductivity k, and viscosity ν. Considering a general case where the distribution function is the solution of equation 2.42 the particle current density is

$$\Gamma = \iiint\limits_{all\ v} f_e v d^3 v \tag{2.43}$$

In the case of free diffusion, this net current density becomes necessarily proportional to the concentration gradient, the constant of proportional being by definition the diffusion coefficient D.

$$\Gamma_{dif} = -D\nabla n \tag{2.44}$$

Under the effect of an externally applied force, the particles acquire a drift velocity v_d and are said to have a mobility b. If the external force is due to an applied electric field $\vec{E}$, the resulting drift velocity of the particles can readily be obtained from the equation of balance of forces:

$$v_d = \frac{e}{M}\left\langle \frac{1}{\nu_c} \right\rangle E \tag{2.45}$$

where $\left\langle \frac{1}{\nu_c} \right\rangle$ is the inverse the collision frequency averaged over the distribution function. The mobility is defined as the ratio of the drift velocity over the electric field, $b = v_d/E$, and, comparing this equation to equation 2.44, it is found that

$$b = \frac{e}{M}\left\langle \frac{1}{\nu_c} \right\rangle \tag{2.46}$$

One of the transport coefficients is the electrical conductivity defined as the net flow of charges in response to an applied electric field. It is found experimentally that the current density produced by an electric field is proportional to it, the constant of the proportionality being by definition the electrical conductivity

$$\vec{J} = \sigma\vec{E} \tag{2.47}$$

which is known as a Ohm's law. Since the electric field is nothing more than a potential gradient, equation 2.47 can be written in a form similar to equation 2.44, or

$$\vec{J} = \sigma\nabla V \tag{2.48}$$

where V is the electrical potential. The current density is expressed in terms of the distribution f_e by

$$\vec{J} = -e\iiint\limits_{all\ v} f_e v d^3 v \tag{2.49}$$

The result of this integration for different types of plasmas determines the value of the conductivity in terms of such quantities as the electronic temperature and density.

Chapter 3

Inductive MHD generator

In this chapter I present the study and the results obtained for an inductive MHD generator. The presented device is an innovative direct energy conversion generator and it can be used for converting thermal energy of fuel and/or thermal energy stored in fluids into electrical energy with a high thermodynamic efficiency and a high rate of energy conversion. The conventional MHD generator has been studied since early of past century [23] as an alternative to the gas turbine based energy conversion. The MHD have the advantage of being a static heat engine. In this machine electricity is produced by passing an ionized gas across a magnetic field. In practice, this kind of machines can only be efficient if the charges concentration in the gas is raised to a level at which the conductivity is adequate. This is usually obtained by heating the gas to a high temperature and seeding it with alkaline metals or with other ionizing elements. The high temperatures needed to ionize the gas is in practice one of the main problems of the known MHD generators but it is not the only one. Two further problems have to be taken into account. The first one concerns the need to have a high magnetic field (about 5T) with the consequent need to use superconducting windings and the second one concerns the deterioration of the electrodes which are in contact with the plasma at high temperature.

The proposed device allows to overcome the typical drawbacks of the conventional MHD generators. In fact the proposed device does not need an external magnetic field to work, but it performs the energy conversion by means

of the induction principle. This is possible thanks to a pulsed ionization of the fluid current, carried out with an electrode dipped in the fluid current, followed by a charge separation with a stationary electric field.

3.1 Physical phenomena Description

The inductive MHD generator here presented can convert the energy from fossil fuel directly into electricity, and for that it can be considered into the direct energy conversion category. As all the energy direct conversion processes, also the inductive MHD generator studied, can convert the thermal energy into electricity without moving parts. As enlighten in the first chapter, the absence of moving parts can improve the efficiency of the conversion, allows one working at temperature higher than conventional processes and this permits to obtain higher efficiency of the energy conversion. The innovation, respect to the conventional MHD generator, is that the external magnetic field is no longer necessary. In fact, the proposed device does not need an external magnetic field to work but the energy conversion is possible thanks to the inductive principle. The working principle of the generator studied is quite simple. A high speed gas enters in the duct where in the first part it is ionized by a pulsating electric discharge. The charges of different sign are separated by using an external electric field. The motion of ionized fluid through an electric field $\vec{E}$ produces on each charge q of the fluid a force $\vec{F} = q\vec{E}$ parallel to the direction of $\vec{E}$ that separate the charges with different sign in the direction perpendicular to the motion of the fluid. Downstream of this process a diaphragm splits the flow in two charges currents, one having an excess of positive charge, the other of negative charge. In this way a pulsating electric current is generated around the diaphragm. The current generated induces an electromotive force in toroidal coils wrapped around a core of very high magnetic permeability placed in the cavity and around the duct.

In figure 3.1 a functional scheme of the proposed generator is shown. The generator is composed of three main sections. A first section is dedicated for the ionization of the inlet fluid, the second one provide the charge separation and finally in the last section the transmission of energy to the electric load takes place.

The ionization of the fluid can be obtained in different ways, in this study it is obtained by means of electrodes powered by a high voltage generator to

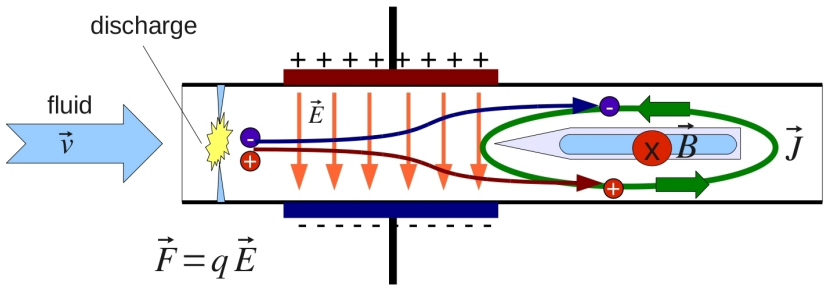

Figure 3.1: Inductive MHD generator functional scheme

generate a electric pulsating discharge. A sufficient number of charge carries have to be generated during the discharge in order to obtain a meaningful electrical current. The ionization of the fluid has an important role in the performance of the generator. The electrode must be in contact with the fluid and placed in the first part of the duct and connected to the high voltage pulse generator. The high voltage generator must be properly programmed to choose the optimal parameters of discharge generation.

In the second section the apparatus for the separation of the charges is composed of two plates of a capacitor externally powered by a DC high voltage generator. The external electric field has to be calibrated in such a way the charge carries are separated without to be blocked in the internal side of the duct (the voltage applied to the capacitor plates must be able to separate the positive and negative charges produced from the electric discharge, but at the same time, it should not be so high to cause a block of them on the inner walls of the duct). At the end of the separation process the fluid is split in two currents, one having an excess of positive charge and the other one negative. The two currents enter in the third section of the generator.

When the fluid current reaches the third section of the generator, where there is the diaphragm, the charge carries are asymmetrically distributed, so that the fluid is split in two electrically unbalanced flows, that give rise to a ring of electric current around the diaphragm (see Figure 3.1). In this section the energy conversion process is carried out, where a part of the energy of the fluid is transferred to the external load. In fact the ring of electric current is time-varying, then induces an electromotive force in a toroidal coil wrapped around

a core of very high magnetic permeability placed in the cavity and around of the duct.

As can be noted, no external magnetic field has to be generated, the positive and negative charges are separated by means of a external electric field and the energy conversion is possible thanks to the inductive process. Furthermore, the electric charge is generated by means of an electric discharge, therefore provided that the pulsing voltage is enough high, the gas can be ionized also at low temperatures. Finally, the plasma and the electric load are magnetically coupled, so that no electrode subject to deterioration is necessary. The above advantages can be translated into economic terms, considering the lower costs for the construction of the generator in study than the conventional MHD generators. In fact, costs are reduced by the absence of a complex and expensive system of superconducting windings. The benefits permitted by this generator can be used, not only to replace the conventional MHD generators, but also in other applications for direct energy conversion.

3.2 Apparatus description

The device under study has a square section with sides of 110 mm and a length of 234 mm as shown in figure 3.2. The device consists of: high voltage pulse generator, discharge electrodes, DC high voltage generator, capacitor plates, diaphragm, magnetic circuit and the secondary winding. The high voltage pulsing generator connected with the discharge electrodes form the necessary components to generate the electric discharge. The DC high voltage generator is connected to the capacitor plates and these allow the separation charges process. The diaphragm, placed inside of the duct, has a airfoil shape and has internal cavity with rectangular section. The particular airfoil shape allows one to limit the drag and to abate the internal pressure drop. In the inner part of the diaphragm (cavity) and around the duct is placed a magnetic circuit core with high magnetic permeability. The magnetic circuit core is made up of two closed loop paths containing a magnetic flux generated by time varying current, created after charges separation, around the diaphragm. Finally there is a secondary winding wrapped with the external core and connected to the external load.

All these components are necessary for functioning of generator. The duct is connected upstream with the flow coming from the combustion chamber

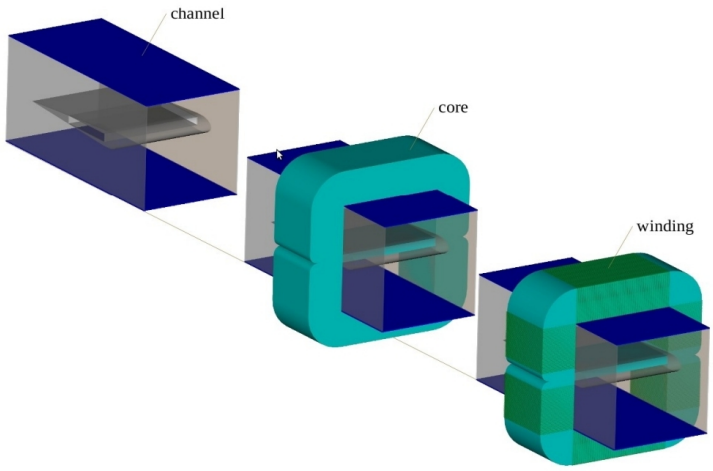

Figure 3.2: Experimental device

and downstream with the exhaust gas system.

3.3 The energy conversion

The physical process of energy conversion occurs in the third section of the generator. Here the physical principle is similar to the conventional transformer where the electrical energy is transferred from the primary winding to the secondary winding through the inductive linkage. In this case the calculation of the inductive electromotive force has been obtained by considering an equivalent circuit [3] where the primary winding is due to the motion of the electric charge around the diaphragm (current ring) and the secondary consists in a number of windings distributed in all other branches of the magnetic circuit as shown in the figure 3.3.

A varying current in the primary winding creates a varying magnetic flux in the transformer's core, which is linked with the secondary winding. This varying magnetic flux induces a varying electromotive force in the secondary winding. If a load is connected to the secondary, an electric current will flow in the secondary winding and an electrical energy will be transferred from the primary circuit through the transformer to the load.

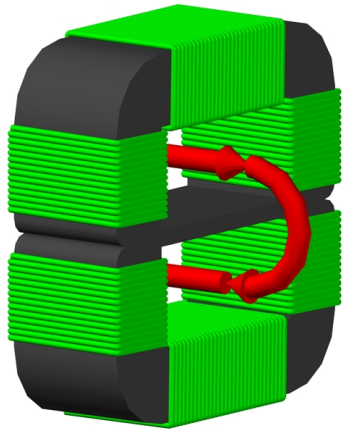

Figure 3.3: 3D magnetic circuit scheme

The figure 3.4 displays the equivalent magnetic circuit studied to calculate the voltage generated to the head of the secondary when this is open.

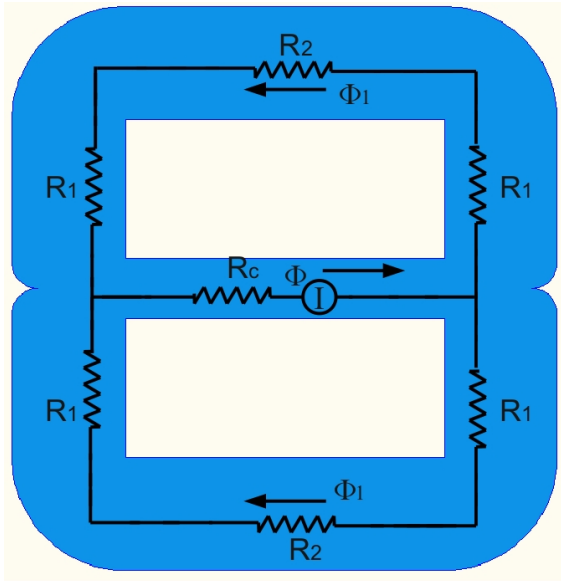

Figure 3.4: equivalent magnetic circuit

The magnetic circuit studied is made up of two closed loop paths. The Hopkinson's law said:

$$F = \phi R_m \tag{3.1}$$

where F is the magnetomotive force, ϕ is the magnetic flux and R is the magnetic reluctance. The reluctance of a magnetically uniform magnetic circuit element can be calculated as:

$$R = \frac{l}{\mu A} \tag{3.2}$$

where l is the length of the element, μ is the permeability of the material and A is the cross-section area of the circuit. Neglecting the intermediate steps, has been evaluated the flux concatenated with the secondary winding:

$$\phi_c = \frac{N_s \cdot I}{2R_1 + R_2 + 2R_c} \tag{3.3}$$

where respectively N_s is the number of turns of wire in the secondary winding, I is the ring of fluid current around the diaphragm and R_1, R_2 and R_c are the magnetic reluctances in the circuit elements. In this way the electromotive force generated at the head of secondary winding is given by:

$$EMF = \frac{d\phi_c}{dt} \tag{3.4}$$

The electric current in the secondary winding determines the reaction field, which slows down the charge carries of the primary. This allows the energy conversion. In fact, the current slowdown in the fluid determines a gas expansion as it happens in a conventional gas turbo-generator, giving part of its internal energy to the load. The inductive generator has a Brayton power cycle, similar to that of gas turbines. However, unlike the gas turbine, there are not moving mechanical parts. All Bryton cycles are heat engine and their ideal cycles have an ideal efficiency equal to ideal Carnot cycle efficiency. The higher the inlet temperature, the greater the ideal efficiency of Brayton cycle. The absence of moving parts allows the inductive generator to withstand temperatures such that of combustion chamber, so inherently an inductive MHD generator has a higher potential capability for energy efficiency.

The figure 3.5 shows the energy balance in the conversion process. Not all the energy input is transferred to the external load. Some of the energy is used

in the conversion process and other part is available at the output. The global efficiency of energy conversion can be increased considering a multi-stages system, in this way can be convert more energy.

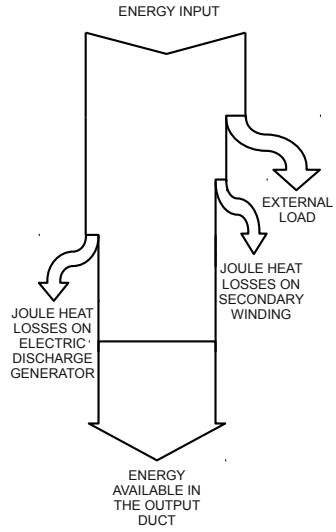

Figure 3.5: Inductive MHD generator functional scheme

Considering a duct with adiabatic walls a part of the total energy available at the energy conversion is dissipated in the windings, core and surrounding structures. Usually these losses are very small and can be neglected. Different consideration have to be done for the energy needed in the discharge process. In fact, part of this energy is not lost but available in the fluid as internal energy.

3.4 Modeling of the inductive MHD generator

The mathematical model time dependent of plasma flow in an electric field is described by system of coupled (nonlinear) equations, consisting of Poisson's equation for electric potential, Navier-Stokes equation for fluid flow,

charge transport equation for electric charge density and the conservation energy equation.

Electrohydrodynamic flow induced by electric discharge is described by the following equations.

The electric potential V is governed by the Poisson's equation

$$\nabla^2 V = -\frac{q}{\varepsilon_0} \tag{3.5}$$

where q is the space charge density and ε_0 is the dielectric permittivity of the free space.

The electric potential is defined from electric field intensity $\vec{E}$ as

$$\vec{E} = -\nabla V \tag{3.6}$$

Electric current in the drifting zone is a combination of three effects: conduction (motion of charges under electric field relative to entire flow), convection (transport of charges with flow), and diffusion. Therefore, current density $\vec{J}$ is given by

$$\vec{J} = \mu_E \vec{E} q + \vec{U} q - D\nabla q \tag{3.7}$$

where μ_E is the charge mobility in a electric field, $\vec{U}$ is the velocity vector of flow, and D is the diffusion coefficient of charges. Current continuity condition gives equation for current density

$$\frac{\partial q}{\partial t} + \nabla \cdot \vec{J} = 0 \tag{3.8}$$

The fluid dynamic part of the problem is described by Navier-Stokes equation and continuity equation:

$$\rho \frac{\partial \vec{U}}{\partial t} + \rho \vec{U} \cdot \nabla \vec{U} = \nabla \cdot [-p\bar{\bar{I}} + \eta(\nabla \vec{U} + (\nabla \vec{U})^T)] - q\nabla V + \vec{J} \times \vec{B} \tag{3.9}$$

$$\frac{\partial \rho}{\partial t} + \nabla \cdot (\rho \vec{U}) = 0 \tag{3.10}$$

where ρ is the flow density, p is the flow pressure, η is the gas dynamic viscosity and $\vec{B}$ is the magnetic induction. By substituting expression for current density 3.7 into equation 3.8 and taking into account definition of electric potential 3.6, we can obtain the following charge transport equation

$$\frac{\partial q}{\partial t} + \nabla \cdot (-D\nabla q - \mu_E \nabla V q + \vec{U} q) = 0 \tag{3.11}$$

where q is the space charge density, D denote the diffusion coefficient, μ_E is the mobility of charge carriers and $\vec{U}$ is the velocity vector.

The conservation of energy can be described by the following equation:

$$\rho \frac{d\hat{u}}{dt} = -p\nabla \cdot \vec{U} + \nabla \cdot (k\nabla T) + \vec{J} \cdot \vec{E} \tag{3.12}$$

where $\hat{u}$ is the internal energy, k the heat conductivity coefficient and T the temperature of the fluid. In the case of ideal gas, with $p/\rho = RT$ and $\hat{u} = c_v T$, the energy conversion become:

$$\rho c_v \frac{dT}{dt} = -p\nabla \cdot \vec{U} + \nabla \cdot (k\nabla T) + \vec{J} \cdot \vec{E} \tag{3.13}$$

where c_p is the heat capacitance of the gas at constant pressure.

3.5 COMSOL application mode

In this section I present the software COMSOL Multiphysics and the main application mode used to solve the electrohydrodynamic equations reported in the preview section.

COMSOL Multiphysics is a powerful interactive environment for modeling and solving all kinds of scientific and engineering problems based on partial differential equations (PDEs). To solve the PDEs, COMSOL Multiphysics uses the proven finite element method (FEM). The software runs the finite element analysis together with adaptive meshing and error control using a variety of numerical solvers. The package provides a number of application modes that consist of predefined templates and user interfaces already set up with equations and variables for specific areas of physics.

The applied physical model to study the electrohydrodynamic equations problem can be divided into three main modules:

- electrostatic stationary model to evaluate electrostatic field;
- fluid flow simulation model based on Navier-Stokes equation (NS);

- and convection and diffusion simulation model to evaluate charge diffusion.

In the following section will be described the COMSOL application physical model. For each model the equations and the boundary condition usable will be described.

3.5.1 Electrostatic Application mode

Modeling of static electric fields is carried out using the electric potential V. Under static conditions, the electric potential V is defined by the equivalence

$$\vec{E} = -\nabla V \tag{3.14}$$

Considering this equation with the constitutive relationship $\vec{D} = \varepsilon_0 \vec{E} + \vec{P}$ between $\vec{D}$ and $\vec{E}$, it is possible to represent Gauss'law as Poisson's equation

$$-\nabla \cdot (\varepsilon_0 \nabla V - \vec{P}) = \rho \tag{3.15}$$

To solve the problem we have to set the propriety of the media and the boundary conditions. It is possible to set the following boundary conditions:

The electric-displacement boundary condition

$$\vec{n} \cdot \vec{D} = \vec{n} \cdot \vec{D}_0 \tag{3.16}$$

The surface charge boundary condition

$$-\vec{n} \cdot \vec{D} = \rho_s \tag{3.17}$$

The zero surface charge boundary condition

$$-\vec{n} \cdot \vec{D} = 0 \tag{3.18}$$

The electric-potential boundary condition

$$V = V_0 \tag{3.19}$$

The ground boundary condition

$$V = 0 \tag{3.20}$$

The continuity boundary condition

$$\vec{n} \cdot (\vec{D}_1 - \vec{D}_2) \tag{3.21}$$

3.5.2 The turbulent application mode

The Navier-Stokes equations describe the mass and momentum transport. These equations can also be used for turbulent flow simulations, although that requires a large number of elements to capture all the dynamics of the flow. An alternative is to consider the average equations, resulting in a hierarchy of equations known as "closure relations", of which the eddy viscosity approach is the most common one. The software COMSOL Multiphysics uses two of such closure scheme: $k-\varepsilon$ [27] and $k-\omega$. Both application modes assume that the flow is incompressible and that the fluid is Newtonian. The flow is than in theory guided by the incompressible Navier-Stokes equations:

$$\rho \frac{\partial \vec{U}}{\partial t} + \rho(\vec{U} \cdot \nabla)\vec{U} = \nabla \cdot [-p\bar{\bar{I}} + \eta(\nabla \vec{U} + (\nabla \vec{U})^T)] + \vec{F} \tag{3.22}$$

$$\nabla \cdot \vec{U} = 0 \tag{3.23}$$

where

- ρ is the density (kg/m^3)
- $\vec{U}$ is the velocity vector (m/s)
- p is the pressure (Pa)
- $\vec{F}$ is the body force vector (N/m^3)

Fundamental to the analysis of fluid flow is the Reynolds number:

$$Re = \frac{\rho U L}{\eta} \tag{3.24}$$

where U denote a velocity scale, and L denotes a characteristic length.

The $k-\varepsilon$ model is one of the most used turbulence models for industrial applications. This model introduces two additional transport equation and two dependent variables: the turbulent kinetic energy, k, and the dissipation rate of turbulent energy, ε. Turbulent viscosity is modelled by

$$\eta_T = \rho C_\mu \frac{k^2}{\varepsilon} \tag{3.25}$$

where C_μ is a model constant.

The transport equation for k can be divided by taking the trace of the equation for the Raynolds stresses:

$$\rho\frac{\partial k}{\partial t} - \nabla\cdot\left[\left(\eta + \frac{\eta_T}{\sigma_k}\right)\nabla k\right] + \rho\vec{U}\cdot\nabla k = \frac{1}{2}\eta_T\left(\nabla\vec{U} + (\nabla\vec{U})^T\right)^2 - \rho\varepsilon \tag{3.26}$$

An equation for ε can be derived in a similar manner.

$$\rho\frac{\partial \varepsilon}{\partial t} - \nabla\cdot\left[\left(\eta + \frac{\eta_T}{\sigma_\varepsilon}\right)\nabla\varepsilon\right] + \rho\vec{U}\cdot\nabla\varepsilon = \frac{1}{2}C_{\varepsilon 1}\frac{\epsilon}{k}\eta_T\left(\nabla\vec{U} + (\nabla\vec{U})^T\right)^2 - \rho C_{\varepsilon 2}\frac{\epsilon^2}{k} \tag{3.27}$$

the model constant in the above equations are determined from experimental data [27] their value are listed in table 3.1.

constant	**value**
C_μ	0.09
$C_{\varepsilon 1}$	1.44
$C_{\varepsilon 2}$	1.92
σ_k	1.0
σ_ε	1.3

Table 3.1: model constant in equation 3.26 and equation 3.27.

In the model we have to set the following sub-domain quantities: ρ, η and $\vec{F}$.

The turbulent application modes have the same boundary types as the Incompressible Navier-Stokes application modes. The boundary condition for the Incompressible Navier-Stokes application modes are grouped into the following types:

- **Wall**

No slip

This is the standard and default boundary condition for a stationary solid wall. The condition prescribes

$$\vec{U} = 0 \tag{3.28}$$

that is, that the fluid at the wall is not moving.

Slip

The slip condition assumes that there are no viscous effects at the slip wall and hence, no boundary layer develops. Mathematically it can be formulated as:

$$\vec{U} \cdot \vec{n} = 0, \qquad \vec{t} \cdot [-p\bar{\bar{I}} + \eta(\nabla\vec{U} + (\nabla\vec{U})^T)]\vec{n} = 0 \tag{3.29}$$

Sliding Wall

This boundary condition assumed that the surface is sliding in its tangential direction. This boundary condition has different definitions in the different space dimensions. In 2D and Axial Symmetry the velocity is given as a scalar U_w and the condition prescribes

$$\vec{u} \cdot \vec{n} = 0 \qquad \vec{u} \cdot \vec{t} = U_W \tag{3.30}$$

where $\vec{t} = (-ny, nx)$ for 2D and $\vec{t} = (-nz, nr)$ for axial symmetriy.

In 3D the velocity is set equal to a given vector u_W projected onto the boundary plane

$$\vec{u} = \vec{u}_W - (\vec{n} \cdot \vec{u}_W)\vec{n} \tag{3.31}$$

- **Inlet and outlet**

This boundary type contains different ways to specify condition on a boundary where the fluid is supposed to enter or exit the domain. The typical boundary type are:

Velocity

This boundary condition has two ways to specify an inlet or outlet velocity. The first one is to set the velocity equal to a given vector u_0 :

$$\vec{u} = \vec{u}_0 \tag{3.32}$$

The other is to specify a normal inflow/outflow velocity:

$$\vec{u} = \vec{n}U_0 \tag{3.33}$$

Pressure

This boundary condition prescribes only a Dirichlet condition for the pressure

$$p = p_0 \tag{3.34}$$

No viscous stress

Prescribe vanishing viscous stress

$$\eta(\nabla\vec{U} + (\nabla\vec{U})^T)\vec{n} = 0 \tag{3.35}$$

- **Symmetry boundary**

Symmetry boundary conditions are used when the physical geometry of interest, and the expected pattern of the flow solution, have mirror symmetry. They can also be used to model zero-shear slip walls in viscous flows. Symmetry boundary condition prescribes no penetration and vanishing shear stresses

$$\vec{u}\cdot\vec{n} = 0 \qquad \vec{t}\cdot[-p\bar{\bar{I}} + \eta(\nabla\vec{U} + (\nabla\vec{U})^T)]\vec{n} = 0 \tag{3.36}$$

- **Open boundary**

This boundary type can be used on boundaries that are open to large volumes of fluid. Fluid can both enter and leave the domain on boundaries with this type of condition.

No viscous stress

it can be considered by vanishing viscous stress:

$$\eta(\nabla\vec{U} + (\nabla\vec{U})^T)\vec{n} = 0 \tag{3.37}$$

Normal stress

In this case the total stress on the boundary is set equal to a stress vector of magnitude , f_0 oriented in the negative normal direction:

$$(-p\bar{\bar{I}} + \nabla\vec{U} + (\nabla\vec{U})^T)\vec{n} = -f_0\vec{n} \tag{3.38}$$

This implies that the total stress in the tangential direction is zero.

- **Stress**

This type of boundary condition represents a very general class of conditions also known as traction boundary conditions.

General stress

The total stress on the boundary is set equal to a given stress $\vec{F}$:

$$(-p\bar{\bar{I}} + \nabla\vec{U} + (\nabla\vec{U})^T)\vec{n} = \vec{F} \tag{3.39}$$

Normal stress

The total stress on the boundary is set equal to a given stress $\vec{F}$:

$$(-p\bar{\bar{I}} + \nabla\vec{U} + (\nabla\vec{U})^T)\vec{n} = f_0\vec{n} \tag{3.40}$$

This implies that the total stress in the tangential direction is zero.

Normal stress, Normal flow

In addiction to the stress condition set in the normal stress condition, this condition also prescribes that there must be no tangential velocities on the boundary:

$$(-p\bar{\bar{I}} + \nabla\vec{U} + (\nabla\vec{U})^T)\vec{n} = f_0\vec{n} \qquad \vec{t}\cdot\vec{u} = 0 \tag{3.41}$$

All boundary conditions need additional conditions for the turbulence transport equations.

The **slip boundary condition** assumes that there is no viscous interaction between the wall and the fluid. In addition to the conditions prescribed for the momentum equations, this boundary condition also prescribes

$$\vec{n}\cdot\left(\left(\eta + \frac{\eta_T}{\sigma_k}\right)\nabla k - \rho\vec{U}k\right) = 0 \tag{3.42}$$

$$\vec{n}\cdot\left(\left(\eta + \frac{\eta_T}{\sigma_\varepsilon}\right)\nabla \varepsilon - \rho\vec{U}\varepsilon\right) = 0 \tag{3.43}$$

the value of the constants σ_k and σ_ε are listed in table 3.1.

Logarithmic wall function applied to finite elements assume that the computational domain begins at distance δ_W from the real wall. They also assumed that the flow is parallel to the wall and that the velocity can be described by

$$U^+ = \frac{U}{u_\tau} = \frac{1}{k}\ln\left(\frac{\delta_W}{l^*}\right) + C^+ \tag{3.44}$$

Here U is the velocity parallel to the wall, u_τ is the friction velocity defined by

$$u_\tau = \sqrt{\frac{\tau_W}{\rho}} \tag{3.45}$$

k denote the Karman constant (about 0.42)[6], and C^+ is a universal constant for smooth walls. In the application mode, C^+ is defined as an application scalar variable that has a default value of 5.5. Further, l^* is known as the viscous length scale and is defined by

$$l^* = \frac{\eta}{\rho u_\tau} \tag{3.46}$$

the distance δ_W have to be specified or its equivalent in viscous units, $\delta_W^+ = \delta_W / l^*$. The logarithmic wall functions are formally valid for value of δ_W^+ between 30 and 100.

The boundary condition for k, ε are derived from the assumption that turbulent production equals the dissipation:

$$\nabla k \cdot \vec{n} = 0 \qquad \varepsilon = \frac{{C_\mu}^3/4k^3/2}{k\delta_W} \tag{3.47}$$

Inlet boundaries are the same as described for the incompressible Navier-Stokes, in addition value for the two turbulent quantities need to be specified (k and ε). Alternatively you can specify a turbulent length scale, L_T and a turbulent intensity, I_T. They are related to the turbulent variables by expression

$$k = \frac{3}{2}(|\vec{U}|I_T)^2, \qquad \varepsilon = C_\mu^{3/4}\frac{k^{1/2}}{L_T} \tag{3.48}$$

In the **outlet boundary** and **open boundaries** the convective flux condition are prescribed for the turbulent variables:

$$\vec{n}\cdot\nabla k = 0, \qquad \vec{n}\cdot\nabla\varepsilon = 0 \tag{3.49}$$

The equation for the **symmetric boundary condition** become:

$$(-p\bar{\bar{I}} + (\eta+\eta_T)(\nabla\vec{U} + (\nabla\vec{U})^T))\cdot\vec{t} = 0 \qquad \vec{n}\cdot\vec{U} = 0 \tag{3.50}$$

$$\vec{n}\cdot\left(\left(\eta + \frac{\eta_T}{\sigma_k}\right)\nabla k - \rho\vec{U}k\right) = 0 \tag{3.51}$$

$$\vec{n}\cdot\left(\left(\eta + \frac{\eta_T}{\sigma_\varepsilon}\right)\nabla\varepsilon - \rho\vec{U}\varepsilon\right) = 0 \tag{3.52}$$

3.5.3 PDE mode to solve Charge transport equation

Charge transport equation 3.11 has been solved using the PDE mode Coefficient Form by setting the coefficient value. The PDF model equation in coefficient form is

$$d_a\frac{\partial q}{\partial t} + \nabla\cdot(-c\nabla q - \alpha q + \gamma) + aq + \beta\cdot\nabla q = R \tag{3.53}$$

where

d_a mass coefficient

c diffusion coefficient

α { α_x conservative flux convection factor x component; α_y conservative flux convection factor y component

γ { γ_x conservative flux source term coefficient x component; γ_y conservative flux source term coefficient y component

a absorption coefficient

β $\begin{cases} \beta_x & \text{convection coefficient x component} \\ \beta_y & \text{convection coefficient y component} \end{cases}$

R source term

In COMSOL PDE mode two kinds of boundary conditions can be defined: the Neumann and Dirichlet condition by fixing the following equations

$$\vec{n} \cdot (c\nabla q + \alpha q - \gamma) + qu = g - h^T \mu \quad \text{(Neumann condition)} \tag{3.54}$$

$$hq = r \quad \text{(Diriclet condition)} \tag{3.55}$$

Chapter 4

2D model of the inductive MHD generator

In this chapter I present the simulation results of a simplified 2D inductive MHD generator model considering two main works. Both these works consider the case of secondary winding left open circuit. In the first work the preliminary results of electrostatic, fluid-dynamic and charge transport will be shown and in the second work a study has been done to evaluate and improve the performance of the proposed device.

4.1 The simplified model of a 2D inductive MHD generator

In this section I present the simplified equations needed to describe the elecrohydrodynamic flow which are the basis for the operation of the studied inductive MHD generator. The simplified model, shown below, considers the generator in the case of secondary winding left open circuit. In these operating conditions it is possible to study a simplified electrohydrodynamic model. The simplified model is obtained and studied using the equations from the section 3.4 and considering the following assumptions:

- The three physical models are solved separately; firstly the solution is obtained for the electrostatic and fluid-dynamic modules. In this way the velocity field and the electric field are calculated and used as source terms to solve the charge transport equation;
- In solving the electrostatic model the charge density has been neglected. This corresponds to neglect the effect of electric fields caused by the electric charges particle;
- In the Navier-Stokes equation the body forces ($-q\nabla V + \vec{J} \times \vec{B}$) is neglected. In the case studied, with left open circuit, the magnetic field of reaction is equal to zero. Furthermore, considering a very small concentration of charge q in the fluid the body force $-q\nabla V$ can be neglected;
- considering a gas flow with a low Mach number the mass density of a fluid can be considered to be constant, regardless of pressure variations in the flow. For this reason the flow can be considered to be incompressible. In this way the continuity equation can be reduced to $\nabla \cdot \vec{U} = 0$;
- under the conditions of the secondary circuit open, the process takes place without the transfer of energy. In these condition, to evaluate the electrohydrodynamic flow, it is possible to neglect the energy equation.

According to the approximations model, the equations used to describe the electrohydrodynamic flow inside the channel of the inductive MHD generator are:

$$\nabla^2 V = 0 \tag{4.1}$$

$$\rho \frac{\partial \vec{U}}{\partial t} + \rho \vec{U} \cdot \nabla \vec{U} = \nabla \cdot [-p\bar{\bar{I}} + \eta(\nabla \vec{U} + (\nabla \vec{U})^T)] \tag{4.2}$$

$$\nabla \cdot \vec{U} = 0 \tag{4.3}$$

$$\rho \frac{\partial k}{\partial t} - \nabla \cdot \left[\left(\eta + \frac{\eta_T}{\sigma_k} \right) \nabla k \right] + \rho \vec{U} \cdot \nabla k = \frac{1}{2} \eta_T \left(\nabla \vec{U} + (\nabla \vec{U})^T \right)^2 - \rho \varepsilon \tag{4.4}$$

$$\rho\frac{\partial\varepsilon}{\partial t}-\nabla\cdot\left[\left(\eta+\frac{\eta_T}{\sigma_\varepsilon}\right)\nabla\varepsilon\right]+\rho\vec{U}\cdot\nabla\varepsilon=\frac{1}{2}C_{\varepsilon1}\frac{\epsilon}{k}\eta_T\left(\nabla\vec{U}+(\nabla\vec{U})^T\right)^2-\rho C_{\varepsilon2}\frac{\epsilon^2}{k} \quad (4.5)$$

$$\frac{\partial q}{\partial t}+\nabla\cdot(-D\nabla q-\mu_E\nabla V q)+\vec{U}\cdot\nabla q=0 \quad (4.6)$$

The equation 4.1 is the Laplace's equation for electrostatic; the equations 4.2 and 4.3 describe the Navier-Stokes equation and continuity equation for incompressible flow. In addition of these equations have been added the turbulent kinetic energy equation, k 4.4, and the dissipation energy equation, ε 4.5. The last equation 4.6 is the transport charge equation. These equation has been solved by using COMSOL multiphysics by setting the electrostatic application mode, the turbulent $k-\varepsilon$ application mode, and the PDE application mode.

4.2 Feasibility analysis of the inductive MHD generator

In this section a preliminary study and analysis of a inductive MHD generator is presented. The numerical model will be described and the preliminary results of electrostatic, fluid-dynamic and charge transport will be shown.

4.2.1 Numerical simulation space model

In this study a 2D configuration model has been used. The volume under control has a rectangular shape with height of 110 mm and a length of 234 mm and it has been divided into eight sub-domains. The inductive MHD generator numerical simulation space, sub-domain, boundaries, and mesh are shown in the figure 4.1.

In the numerical simulation space three main components can be identified: the discharge region, the charge separation region and the diaphragm region. The discharge region is a circular area placed in the first part of the channel and it is centred between the upper and lower wall. The electric discharge is represented by the smallest of the two concentric circles. The larger one has been used to define mesh refinement but it does not represent actual boundaries. The region of charge separation is positioned in the first part of

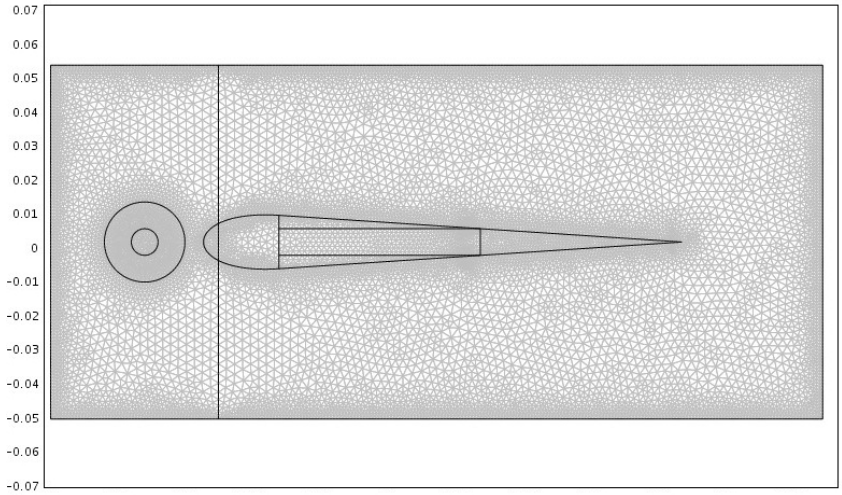

Figure 4.1: Numerical simulation domain and mesh of generator geometry

the channel. The effect of charge separation is performed by means of two parallel plates of a capacitor represented by two edges of the walls above and below the discharge region. In this phase of the study the energy consumption through the electrostatic field in changing the momentum of ions has been neglected. Furthermore we assume that the desired degree of charge separation can be obtained provided that the charge concentration and the electrostatic field are enough high. The diaphragm region is described by five subdomains forming a region with airfoil shape. The numerical simulation space was discretized in approximately 91,000 triangular elements, with the element density being highest in the region around the electrode and the walls.

4.2.2 Electrostatic equation and boundary condition

The electrostatic equation for electrostatic has been solved in COMSOL multiphysics using the electrostatic application mode. The two-dimensional Laplace equation has following form:

$$\frac{\partial^2 V}{\partial x^2} + \frac{\partial^2 V}{\partial y^2} = 0 \tag{4.7}$$

The solution of the equation 4.7 requires appropriate boundary conditions, diversified according to various portions of the boundary that are considered. In reference to the figure 4.1, it is necessary to distinguish between:

- inlet and outlet section;
- capacitor plates;
- walls channel.

Inlet and outlet section

the normal component of the electric field is zero, that is:

$$\vec{n} \cdot \vec{E} = 0 \tag{4.8}$$

This condition consider this boundary at symmetry boundaries where the potential is known to be symmetric with respect to the boundary.

capacitor plates

The two edges of the wall, that represent the capacitor plates, are set with the electric potential boundary condition.

$$V = V_{MAX} = 50[kV] \tag{4.9}$$

$$V = V_{MIN} = 0[kV] \tag{4.10}$$

where V_{MAX} is the electrical potential in the positive capacitor plate and V_{MIN} is the electric potential in the negative capacitor plate.

Walls channel

To the other walls of the channel a symmetry boundary condition has been considered where:

$$\vec{n} \cdot \vec{E} = 0 \tag{4.11}$$

in all this boundary the normal component of the electric field is zero.

4.2.3 Fluid-dynamic equation and boundary condition

The Navier-Stokes equations for turbulent flow (4.2, 4.3, 4.4 and 4.5) have been solved in COMSOL using the turbulent application mode.

In order to solve the Navier-Stokes equations boundary conditions in **inlet section**, **outlet section** and on the **inner walls** of the channel are required.

Inlet section

In the inlet section a normal inflow velocity has been assigned:

$$\vec{U} = \vec{n} \cdot U_0 \tag{4.12}$$

where U_0 has been set equal to 200[m/s].

outlet section

At the outlet section a pressure boundary condition has been used. This condition prescribe a Dirichlet condition for the pressure:

$$p = p_0 \tag{4.13}$$

where p_0 is the pressure imposed equal to 1 [atm].

inner walls

A logarithmic function has been used for all inner channel walls. This type of boundary condition use an empirical relation between the value of velocity and wall friction that replaces the thin boundary layer near the wall. Such relations are accurate for high Reynolds numbers and situations where pressure variations along the wall are not very large.

4.2.4 Charge transport equation and boundary condition

The charge transport equation has been solved in COMSOL using the PDE application mode (section 3.5.3). In this case it is necessary to set the coefficient reported in the PDE equation 3.53. The mass coefficient d_a has been set to the default value equal to 1. The conservative flux term γ and absorption coefficient a have been set equal to zero. The source term R has been used

to model the electric discharge. This term has been set by using the equation that will be reported in the following section 4.2.5. It has been set in the subdomain that describe the discharge region. The conservative flux convection factor has been set to take into account the drift motion of the charge due to the interaction with the electric field. This quantity is proportional to the product of charge mobility μ_E and the electric field $\vec{E}$:

$$\alpha = \mu_E \vec{E} \qquad \begin{cases} \alpha_x = \mu_E E_x \\ \\ \alpha_y = \mu_E E_y \end{cases} \tag{4.14}$$

considering that $\vec{E} = -\nabla V$ the solution is obtained solving the equation 4.7. The convection coefficient β takes into account the motion of the charges that are transported by the fluid. This coefficient is a velocity dimension and has been set equal to the velocity obtained from the solution of the Navier-Stoke equation, then

$$\beta = \vec{U} \qquad \begin{cases} \beta_x = U_x \\ \\ \beta_y = U_y \end{cases} \tag{4.15}$$

For the charge transport equation a zero diffusive flux condition is set on all boundaries except for the outlet surface where convective flux diffusion is imposed.

4.2.5 Charge generation region

Charge generation by electric discharge can be modeled by applying appropriate time varying charge concentration. The energy required for this discharge in this phase of the study has been neglected as the generator has been considered ideal. On the basis of the experimental data retrived from the literature [26], it can be assumed that the charge carries concentration, due to the discharge, is about $10^{14} n_e/cm^3$. The total number of the charges is assumed to be about $2 \cdot 10^{15}$, i.e., it has been assumed that 10 cm^3 are involved in the discharge process. The charge of the same sign is then $n_e \cdot e = 1.610^{-4} C$. The generation of the charge by means of the electrode is modelled injecting a time varying flow of positive and negative charge carriers. In the volume of

the electric discharge a space charge volume density is applied by setting the Reaction rate parameter as follows:

$$R = \frac{C_R}{\sqrt{2\pi \cdot \sigma^2}} \left[e^{\frac{(t-t_1)^2}{2\cdot\sigma^2}} + e^{\frac{(t-t_2)^2}{2\cdot\sigma^2}} \right] \tag{4.16}$$

where:

- C_R is the maximum charges concentration in the time;
- σ is the time constant of charge diffusion;
- t_1 and t_2 are the time interval between two consecutive discharges.

The time interval between t_1 and t_2 is stated in such a way the interference between two consecutive discharges is negligible. The figure 4.2 shows the time variation of R.

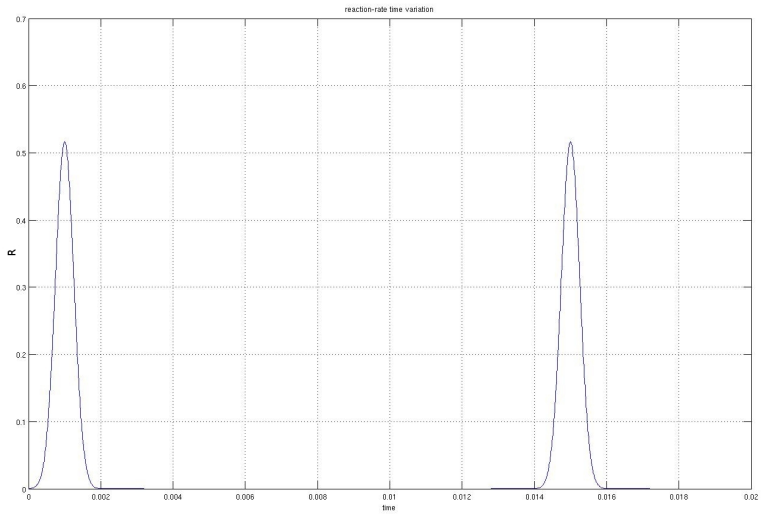

Figure 4.2: Time variation of R

The charges repulsion effect has been taken into account by increasing the value of the diffusion coefficient obtained by comparing the diffusion velocity of peripheral particles with the velocity of the same particles due to the

interaction with the charge distribution. Therefore, the diffusion that without charges interaction would be $\mu = 5 \cdot 10^{-5} m^2/s$ has been corrected with $\mu = 2,1208 \cdot 10^{-4} m^2/s$ taking into account the mobility of the charge carries. The relative dielectric permittivity of the gas is assumed equal to 1.0.

In order to take into account the effect of the external field on the charge carries, in the sub-domain setting of the convection and diffusion model, a velocity term is added to the drift velocity, which depends on the external electrical field and on the mobility of charges. On the basis of the experimental data available in literature [17], a mobility of $1.8 \cdot 10^{-4} m^2 V^{-1} s^{-1}$ has been assumed.

4.2.6 Simulation Parameter

The model has been run by COMSOL 3.5a separating a module involving the electrostatic and fluid mechanics from a module that treats the charge transport aspects. The first modules have been solved by executing a stationary study, then the results have been used to solve the second module that has been analysed with a transient study. The Direct (PARDISO) method has been adopted to solve the equation system of the stationary modules, and the BDF method for the transient module. For the stationary solver a relative tolerance equal to 10^{-6} has been used to control the convergence and the maximum number of iterations has been set to 100, whereas in the transient analysis the relative tolerance has been set to 0.01 and the absolute one equal to 0.001. Firstly the solution is obtained for the electrostatic and fluid-dynamic modules with the use of stationary solver. In this way the velocity field and the electric field are calculated and used as source terms to solve the charge transport equation where transient interactive solver is used. The electric, charge transport, and fluid-dynamic domains equations were solved using the subdomain modeling parameter values shown in Table 4.1.

4.2.7 Results and discussions

In this section the results obtained from the simulation model of electrohydrodynamic equation are presented. The results are presented for 2D configuration model. Surface plots of the investigate model shown in the following figures 4.3, 4.4, 4.5, 4.6 and 4.7 display the solution of three coupled physical phenomena modelled: electrostatic, fluid dynamic and charge transport. The electric potential map, Figure 4.3, has the highest potential at the surface

Modeling parameter	Value
Relative dielectric permittivity of air, ε_r	1
Charge diffusion coefficient D	$2.12x10^{-4}m^2/s$
Ion mobility coefficient, μ_E	$1.8x10^{-4}m^2/(Vs)$
Density of the fluid, ρ_{fluid}	$1.23kg/m^3$
Dynamic viscosity of the fluid, μ	$1.8x10^{-5}Ns/m^2$

Table 4.1: Sub-domain modeling parameter values used in FEM modeling

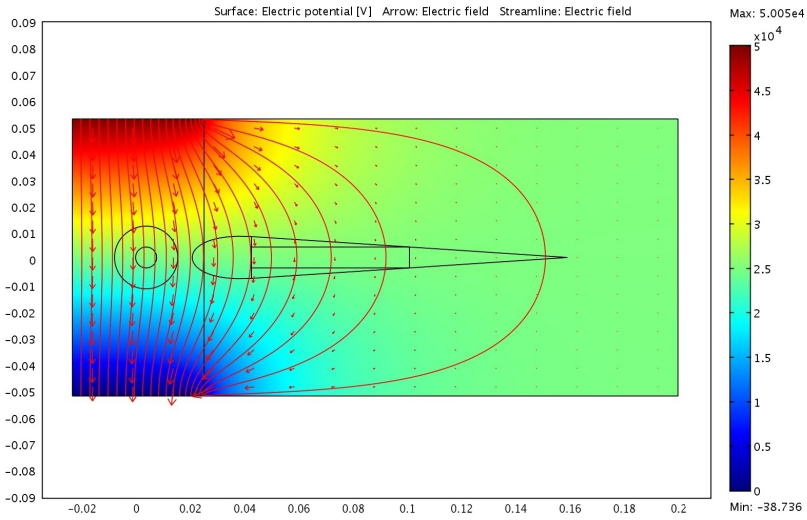

Figure 4.3: Magnitude of electric potential distribution(colour surfaces), electric field lines and electric field vectors (arrows)

of the top capacitor armature and decreasing in magnitude to the bottom one. The velocity field map, Figure 4.4, shows magnitude and streamlines of the gas inside the channel. The figures 4.5, 4.6 and 4.7 display, in the sequential image, the movement of the charge inside of the duct.

As can be observed the charge flow is split in two currents one having excess of positive charge, the other one negative charge.

The calculation of the inductive electromotive force has been obtained by considering an equivalent circuit where the primary winding is due to the mo-

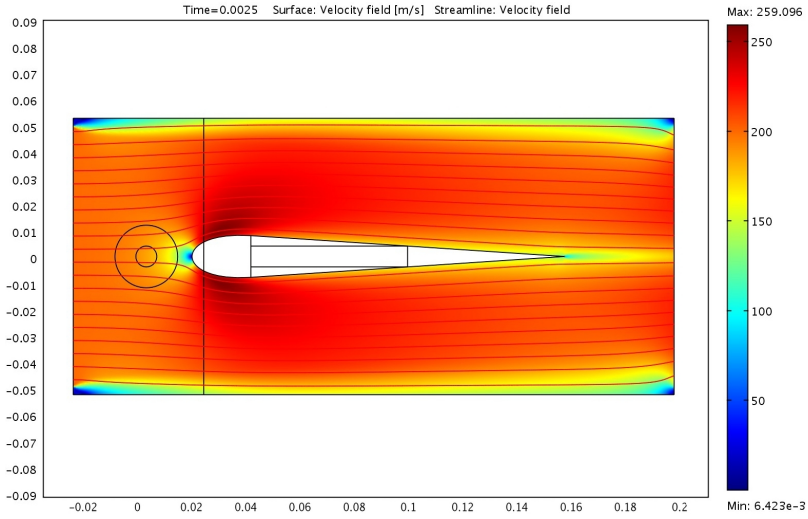

Figure 4.4: Magnitude of gas velocity distribution (colour surfaces), and fluid streamlines

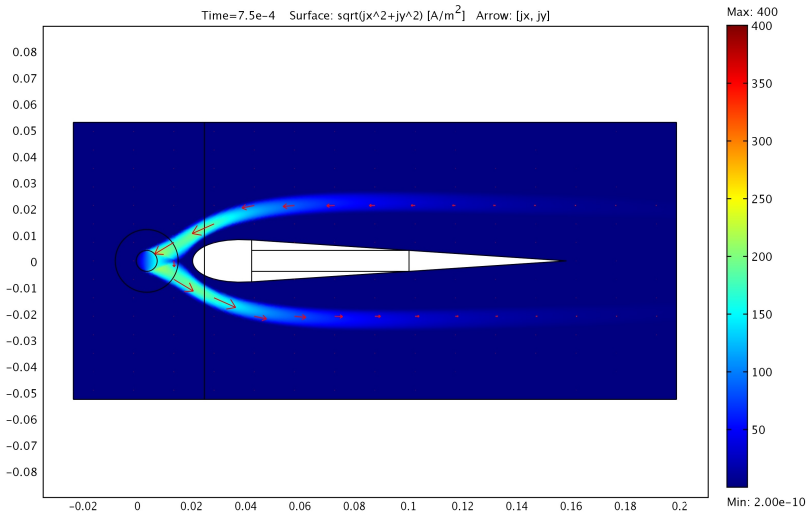

Figure 4.5: Space charge density at the time $0.75ms$

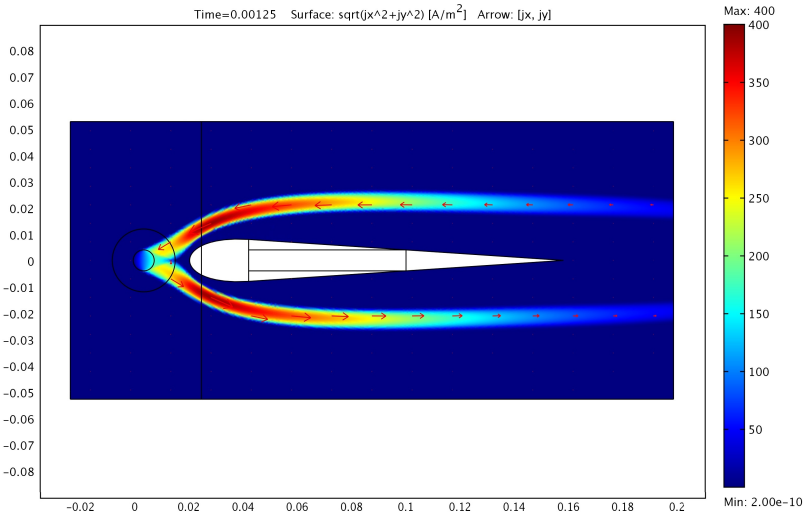

Figure 4.6: Space charge density at the time $1.25ms$

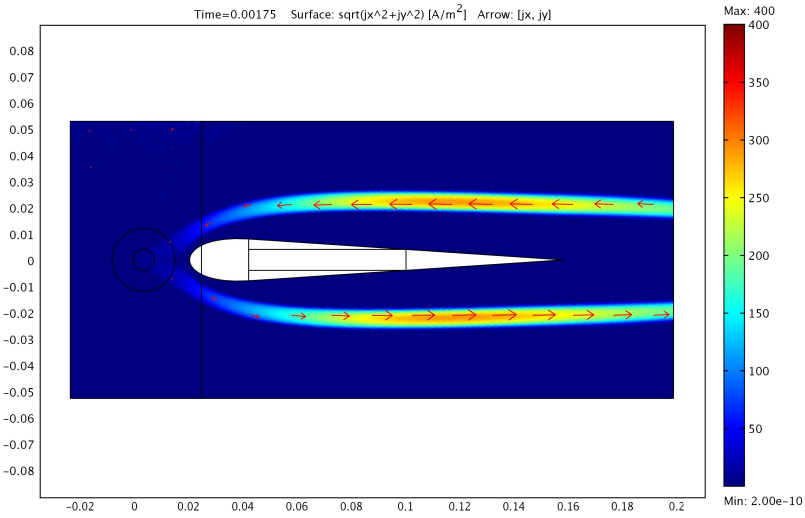

Figure 4.7: Space charge density at the time $1.75ms$

tion of the electric charge in the working fluid and the secondary winding is made up of 8000 coils distributed in all the branches of the magnetic circuit,

except the one internal to the cavity. By considering the secondary winding left open circuit, has been obtained a voltage to the heads of the coil as shown in Figure 4.8. Assuming an adapted load the theoretical maximum power out-

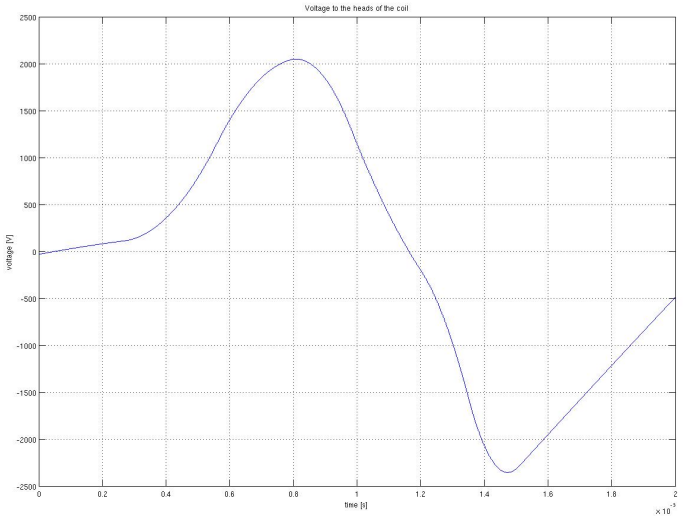

Figure 4.8: Voltage to the heads of the coil

put has been calculated. Known the root mean square voltage at the head of the secondary winding V_{rms}, generated by the induction generator, the output power load can by calculated by:

$$P = V^2{}_{rms} \frac{R_l}{(R_l + R_c)^2} \tag{4.17}$$

where R_c and R_l are respectively the electrical resistance of the secondary winding and the electrical resistance of the external load. In the secondary winding a linear resistance with a value of $0.0269\Omega/m$ has been considered. In this way a resistance of 51Ω has been calculated in the secondary winding. In the case of adapted load, where $R_l = R_c = R$, the theoretical maximum power load is:

$$P = \frac{V^2{}_{rms}}{(4R)^2} \tag{4.18}$$

Considering the equation 4.18 a theoretical maximum power equal to 18kW is obtained.

As mentioned above, the maximum power has been calculated in the case of a load adapted with the assumption of $R_l = R_c$. There are several factors that cause a reduction in performance respect to the theoretical condition, including the increase of external resistive load (R_l) and the time between two consecutive electric discharge t_m. The figure 4.9 shows the trend of the power produced by varying the resistive load and the time between two consecutive electric discharge where t_m is the minimum time range of interference between two discharge pulses. The image shows how the performance decreases with increasing of external resistive load from 51Ω to 800Ω and the time between two discharge pulses ($t_m \div 2.00\,t_m$).

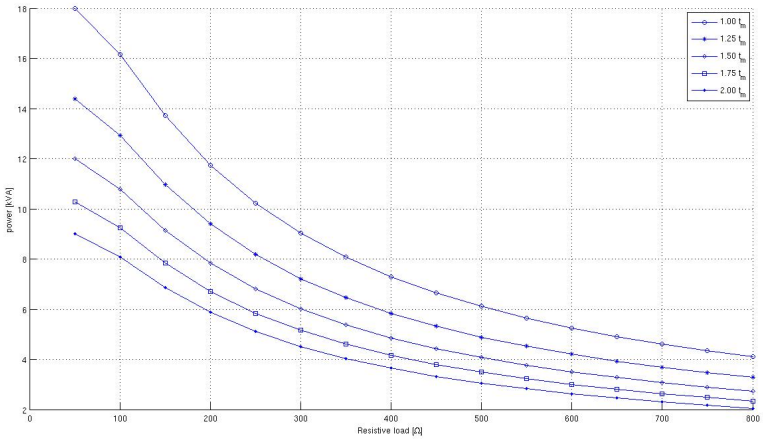

Figure 4.9: Trend of the power produced by varying the resistive load and the time between two consecutive electric discharge

The effect of time between two consecutive pulses is due to the fact that EMF is proportional to the first derivative of the magnetic flux then it is proportional to the frequency of the first and higher harmonics. Increasing the ions velocity gives rise the same effects.

4.3 Sensitivity Analysis of Design Parameters of the inductive MHD Generator

In this section, respect to the preliminary study described in the previous paragraph, a greater attention has been devoted to the profile of device and more heavy working condition has been considered to evaluate and improve the performance of the inductive MHD generator studied. A sensitivity analysis has been performed with respect to several design parameters, such as the geometry of the generator and the inlet velocity of the gas. The performance is evaluated in terms of voltage to the heads of the coil and theoretical maximum power load. The main dimension parameter to take into account is the profile width of the diaphragm and the height of cavity internal to the diaphragm. It has been considered an increasing of dimension with respect to the size assumed in the previous paragraph. Also, 5 working inlet velocities have been considered, from 150 to 250 m/s. Figure 4.10 shows the open circuit

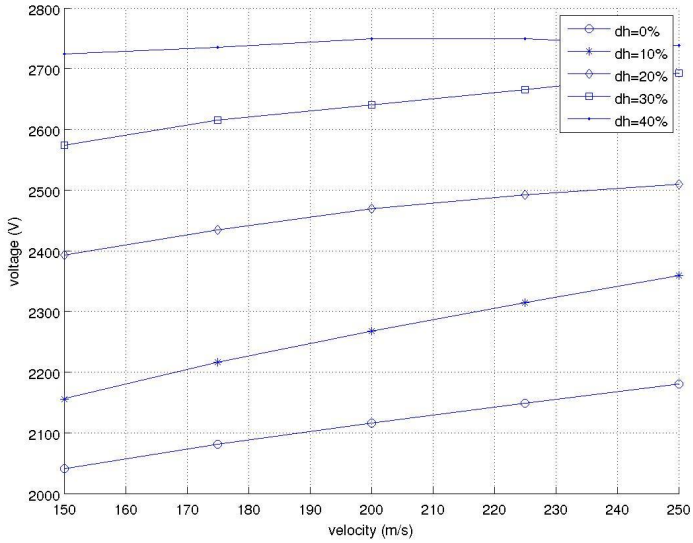

Figure 4.10: Voltage to the heads of the coil, in function of the fluid velocity and for different values of cavity height

voltage obtained by varying both velocity of the working fluid and the height of the cavity internal to the diaphragm. As one can expect, as the flow velocity increases, the inducted voltage rises too, due to the greater velocity of the carriers but also to the fact that the dispersion of the charge clouds take place for a shorter time, so that said clouds remains more concentrated. On its turn, the height of the cavity too determines a greater value of the inducted voltage. In fact the part of core internal to the cavity, represents a bottleneck for the magnetic circuit, and then it limits the value of the magnetic flux. From figures 4.11 and 4.12 can be observed that increasing the size of the magnetic circuit at the

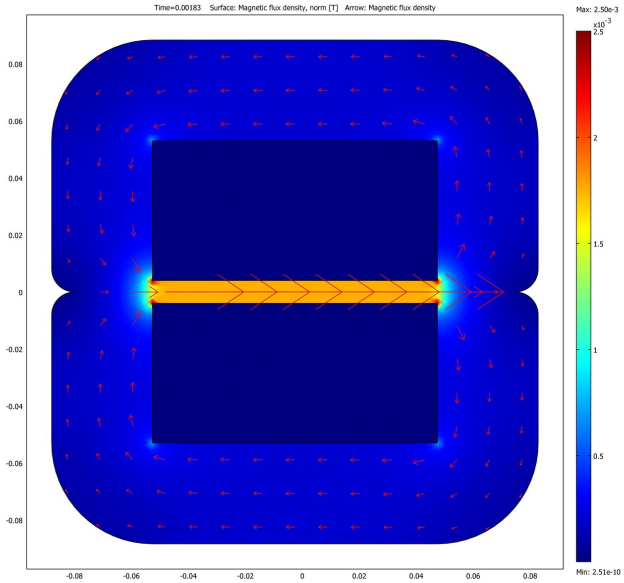

Figure 4.11: Magnetic flux circuit in the case of cavity with minimum section

cavity, the bottleneck phenomenon is less intense, then, in the other path of the magnetic circuit an increase of magnetic flux has been obtained. In Figure 4.13 the maximum power load for the analysed cases is reported. These power values have been calculated with an adapted load, then they depend on the characteristic of the wiring and they are much higher than a possible nominal value. Furthermore, also the time interval between two successive discharges affects the value of the power. In-fact, the working hypothesis is

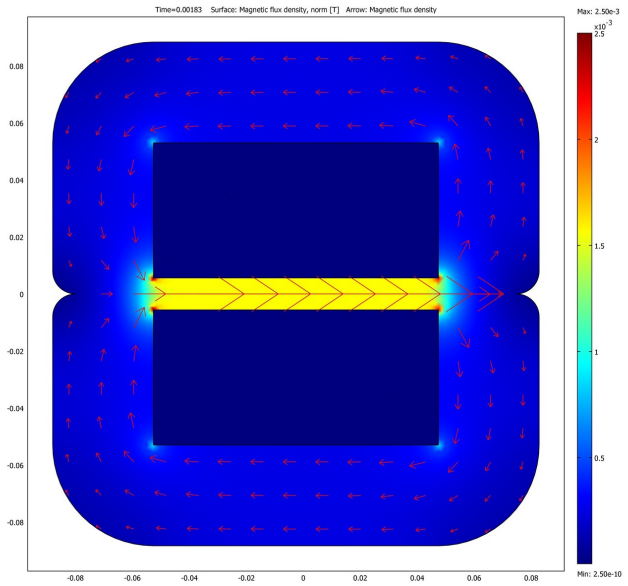

Figure 4.12: Magnetic flux circuit in the case of cavity with maximum section

that the time interval between two successive discharges is equal to the time after which the electrical current in the fluid vanishes, but it would be necessary to wait for a longer interval, in order to allow the charge to be completely removed from the duct, so that the power values could result considerably lower. Therefore, these results depend on several design parameters that have not been considered in the sensitivity analysis performed in this work.

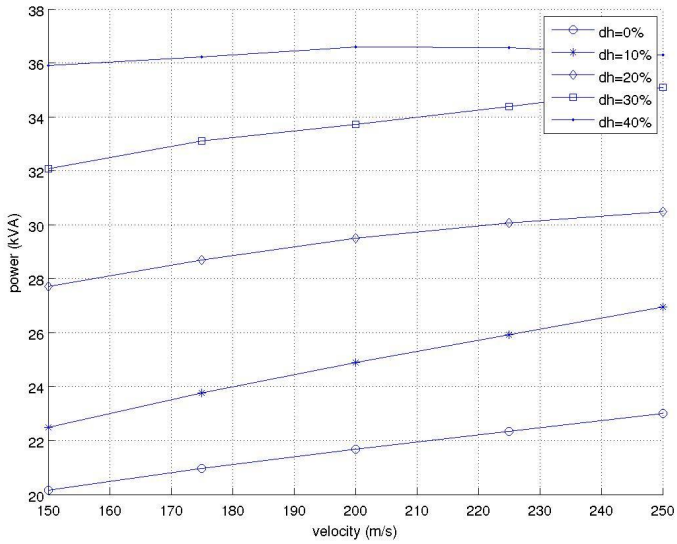

Figure 4.13: Maximum theoretical power retrievable, in function of the fluid velocity and for different values of cavity height

Chapter 5

Conclusions

In this dissertation an innovative MagnetoHydroDynamic (MHD) generator has been studied. The proposed device does not need an external magnetic field to work, but it performs the energy conversion by means of the inductive principle. This is possible thanks to a pulsed ionization of the fluid current, carried out with an electrode dipped in the fluid current followed by a charge separation with a stationary electric field. The presented inductive MHD generator can be used for converting thermal energy directly into electricity with a high thermodynamic efficiency and a high rate of energy conversion. As all direct energy conversion processes, also the inductive MHD generator, can work without moving parts.

In the conventional conversion systems a significant loss of energy occurs in the transition from thermal to mechanical energy (thermodynamic conversion). The performance from the point of view of efficiency of a heat engine is limited by the Carnot cycle. The Carnot efficiency is governed solely by the extreme temperatures of the cycle. The low temperature of the cycle is related to the temperature of the environment, the maximum temperature is rather related to the mechanical resistance of the material at high temperature. Nowadays, gas turbines are the technologies that can work to the highest value of temperature cycle, with values around 1500 K. These technologies are usually used as a topper in a combined cycle gas turbine (CCGT) plant. The Carnot efficiency for a thermal engine that works on those temperatures is about 80%.

In the inductive MHD generator the advantage of having no moving parts allows to work at higher temperatures than a conventional energy conversion. It is possible to work with temperature around 3000K, and a these temperature the maximum theoretical efficiency would be near 90%.

The innovation, respect to the convectional MHD generator, is that the external magnetic field is no longer necessary, the efficiency does not depend on the temperature of the fluid and it is not necessary to use an electrode in contact with the fluid because the plasma and the electric load are magnetically linked. The generator consists of three main sections: the first one allows to ionize the fluid, in the second one the separation of the charges takes place into the fluid and finally the section that allows the coupling with the load at the secondary winding.

In this work has been possible to study the inductive generator by using the Finite Element Analysis (FEM) and a multi-physics approach that has allowed to consider simultaneously fluid-dynamic, electromagnetic and charge transport aspects. The present work has been successfully modeled unsing COMSOL multiphysics, a commercial software package that performs equation-based multiphysics modeling from different physical processes by applying the finite element method.

In the early works the use of this powerful software has allowed us to evaluate the output performance of the generator. In the following works a greater attention has been devote to analyzing and improving the performance of the generator. A sensitivity analysis has been performed with respect to several design parameters, such as the geometry of the generator and the velocity inlet gas flow. In this way it has been possible to evaluate the performance in terms of voltage to the head of the coil and the theoretical maximum power.

Bibliography

[1] V. S. (Vladimir Sergeevich) Bagotï¸ sï¸¡kiiÌ. *Fuel cells : problems and solutions / Vladimir S. Bagotsky.* Hoboken, N.J. : John Wiley Sons, 2009. [cited at p. 11]

[2] Irving Bernard Cadoff and Edward Miller. *Thermoelectric materials and devices / Lectures presented during the course on thermoelectric materials and devices sponsored by the Dept. of Metallurgical Engineering in co-operation with the Office of Special Services to Business and Industry, New York University, N.Y., June 1959 and 1960. Edited by B.Cadoff and E.Miller.* N.Y. : Reinhold Pub. Corp, 1960. [cited at p. 11]

[3] David K. (David Keun) Cheng. *Field and wave electromagnetics / David K. Cheng.* Reading, Mass. : Addison Wesley, 1983. [cited at p. 45]

[4] R. A. (Ronald Alan) Coombe and Ronald Alan Coombe. *Magnetohydrodynamic generation of electrical power / ed. by R.A. Coombe.* Lond. : Chapman and Hall, 1964. [cited at p. 11]

[5] G. T Csanady. *Theory of turbomachines.* New York : McGraw-Hill, 1964. [cited at p. 4]

[6] Rachel E. Jordan Christopher W. Fairall Peter S. Guest P. Ola G. Persson Edgar L Andreas, Kerry J. Claffey and Andrey A. Grachev. Evaluations of the von kÃ¡rmÃ¡n constant in the atmospheric surface layer. *Journal of Fluid Mechanics*, 559:117 – 149, 2006. [cited at p. 57]

[7] Alan L Fahrenbruch and 1927 Bube, Richard H. *Fundamentals of solar cells : photovoltaic solar energy conversion / Alan L. Fahrenbruch, Richard H. Bube.* New York : Academic Press, 1983. [cited at p. 11]

[8] Enrico Fermi. *Thermodynamics / by Enrico Fermi.* New York : Dover Publications, [new ed.] edition, 1956. [cited at p. 21]

[9] Organisation for Economic Co-operation, Development, and International Energy Agency. *World energy outlook to the year 2010 / International Energy Agency.* Paris : IEA : OECD, 1993. [cited at p. 1]

[10] R. J Goldston and 1938 Rutherford, P. H. (Paul Harding). *Introduction to plasma physics / Robert J. Goldston and Paul H. Rutherford.* Philadelphia, PA : Institute of Physics Pub, 1995. [cited at p. 27]

[11] J. H Horlock. *Combined power plants : including combined cycle gas turbine (CCGT) plants / J.H. Horlock.* Oxford [England] ; New York : Pergamon Press, 1st ed edition, 1992. [cited at p. 7]

[12] Naoyuki Kayukawa. Comparisons of mhd topping combined power generation systems. *Energy Conversion and Management*, 41(18):1953 – 1974, 2000. [cited at p. 17]

[13] Naoyuki Kayukawa. Open-cycle magnetohydrodynamic electrical power generation: a review and future perspectives. *Progress in Energy and Combustion Science*, 30(1):33 – 60, 2004. [cited at p. 17]

[14] Rolf Kehlhofer. *Combined-cycle gas steam turbine power plants / Rolf Kehlhofer.* Lilburn, GA : Fairmont Press, 1990. [cited at p. 4]

[15] M. Ali Kettani. *Direct energy conversion / [by] M. Ali Kettani.* Reading, Mass. : Addison-Wesley Pub. Co, 1970. [cited at p. 11]

[16] CleÌment M Lefebvre. *Electric power : generation, transmission, and efficiency / CleÌment M. Lefebvre.* New York : Nova Science Publishers, 2007. Includes index. [cited at p. 11]

[17] E.Hontanon M.Alonso J.P.Borra, J.P.Santos and E.Ramiro. Mobility spectra of air ions generated by corona discharge. *2008 European Aerosol Conference (EAC2008)*, 2008. [cited at p. 69]

[18] Earl W. (Earl Wadsworth) McDaniel. *Collision phenomena in ionized gases / [by] Earl W. McDaniel.* N.Y. : Wiley, 1964. [cited at p. 27]

[19] Roger Messenger and Jerry Ventre. *Photovoltaic systems engineering / Roger A. Messenger, Jerry Ventre.* Boca Raton, Fla. : CRC Press, 2nd ed edition, 2004. [cited at p. 11]

[20] Y. Okuno, T. Okamura, K. Yoshikawa, T. Suekane, K. Tsuji, M. Okubo, T. Maeda, T. Murakami, H. Yamasaki, S. Kabashima, S. Shioda, and Y. Hasegawa. High enthalpy extraction experiments with fuji-1 mhd blow-down facility. *Energy Conversion and Management*, 40(11):1177 – 1190, 1999. [cited at p. 15]

[21] Sumuni Shioda Richard J. Rosa, Charles H. Krueger. Plasmas in mhd power generation. *IEEE Transactions on Plasma Science,*, 19(6):1180 – 1190, 12/1991. [cited at p. 14]

[22] L. A. (Lev Aleksandrovich) Rikhter, EÌ. P Volkov, Vadim Nikolaevich PokrovskiiÌ, and Petr Stepanovich NeporozhniiÌ. *Thermal power plants and environmental control / L.A. Richter, E.P. Volkov, V.N. Pokrovsky ; edited by P.S. Neporozhny ; translated from the Russian by V. Afanasyev.* Moscow : Mir Publishers, rev. from the 1981 russian ed edition, 1984. [cited at p. 15]

[23] Richard J Rosa. *Magnetohydrodynamic energy conversion / Richard J. Rosa.* Washington : Hemisphere Pub. Corp, rev. print edition, 1987. [cited at p. 12, 41]

[24] P. Satyamurthy, T. K. Thiyagarajan, and N. Venkatramani. A conceptual scheme for electrical power generation from nuclear waste heat using liquid metal magnetohydrodynamic energy converter. *Energy Conversion and Management*, 36(10):975 – 987, 1995. [cited at p. 18]

[25] P. Satyamurthy, N. Venkatramani, A. M. Quraishi, and A. Mushtaq. Basic design of a prototype liquid metal magnetohydrodynamic power generator for solar and waste heat. *Energy Conversion and Management*, 40(9):913 – 935, 1999. [cited at p. 19]

[26] M.R. Wertheimer, I. Radu, and R. Bartnikas. Dielectric barrier discharges (dbd) in gases at atmospheric pressure: effect of charge trapping. pages 231 – 234, 2005. [cited at p. 67]

[27] David C Wilcox. *Turbulence modeling for CFD / by David C. Wilcox.* La CaÌnada, Calif. : DCW Industries, 2nd ed edition, 1998. [cited at p. 52, 53]

[28] Mark Waldo Zemansky and Richard Dittman. *Heat and thermodynamics : an intermediate textbook / Mark W. Zemansky, Richard H. Dittman.* New York ; London : McGraw-Hill, 7th ed edition, 1997. [cited at p. 4, 21]

List of Publications Related to the Thesis

Published papers

Conference papers

- Augusto Montisci, Roberto Pintus *"Sensitivity Analysis of Design Parameters of an inductive MHD Generator"* 20th International Symposium on Power Electronics, Electrical Drivers, Automation and Motion, 14-16 June 2010, Pisa, Italy.
- Augusto Montisci, Roberto Pintus *"A Magnetohydrodynamic study of a inductive MHD generator"* The European COMSOL Conference 2009, 14-16 October 2009, Milano, Italy.
- Augusto Montisci, Roberto Pintus *"Feasibility analysis and conceptual design of a inductive MHD Generator"* The 8th International Symposium on Electric and Magnetic Fields, EMF 2009, 26-29 May 2009, Mondovi, Italy.